Journal of Cleaner Production 315 (2021) 128178

Contents lists available at ScienceDirect

Journal of Cleaner Production

journal homepage: www.elsevier.com/locate/jclepro

The influence of particle size on the potential of enhanced basalt weathering for carbon dioxide removal - Insights from a regional assessment

Thomas Rinder *, Christoph von Hagke

University of Salzburg, Department of Geography and Geology, Hellbrunner Straße 34, 5020 Salzburg, Austria

ARTICLE INFO

Handling editor: Zhifu Mi

Keywords:
Negative emissions
Basalt weathering rates
Carbon dioxide removal
Enhanced weathering
Soil amendment
Shrinking core model

ABSTRACT

Enhanced weathering through basalt application on agricultural land represents a proposed strategy for the removal of carbon dioxide from the atmosphere. It has been shown that enhanced weathering is principally feasible on a global scale, but there is still uncertainty with respect to the predicted drawdown in a given timeframe. This information is however vital to evaluate, if enhanced weathering should be further considered as a factor to alleviate the impact of the climate crisis. With this in mind, this article reviews of the current state of research and estimates the CO_2 drawdown for scenarios using basalt powders of different particle size distribution (<100 μm, <10 μm and <1 μm). Calculated with a modified shrinking core model, the amount of powder dissolved within a timeframe of 10 years is approximately 16% (<100 μm), 55% (<10 μm) and 99.9% (<1 μm). This corresponds to a gross CO_2 removal of 0.045 t CO_2 t^{-1} of rock (<100 μm) and 0.153 t CO_2 t^{-1} of rock, (<10 μm). We evaluate our results on regional scale through a case study for Austria, including emissions from mining, comminution, application and transport. Assuming an average distance of 300 km from mine to field, the net CO_2 drawdown decreases to approximately 0.027 t CO_2 t^{-1} of rock (<100 μm) or 0.096 t CO_2 t^{-1} (<10 μm), when rail transport is used. For truck transport, the numbers are reduced to −0.030 t CO_2 t^{-1} of rock (<100 μm) or 0.039 t CO_2 t^{-1} (<10 μm), respectively. Accordingly, at the current CO_2 intensity, transport related emissions may cancel out any drawdown if grain sizes (<100 μm) are used. Our estimates suggest that enhanced weathering will only significantly contribute to net CO_2 drawdown if grain sizes (<10 μm) are used. Under these conditions the large-scale application of particles with a diameter <10 μm may remove about 2% of Austria's annual Greenhouse gas emissions. We discuss challenges towards this goal, including the enormous amounts of rock needed and the energy requirement related to grinding, as well as uncertainties related to actual field weathering rates. Those uncertainties hinder the precise quantification of CO_2 drawdown as of now. While enhanced weathering remains a promising path for climate change mitigation, further research at laboratory and field scale is required to put this technology to optimal use.

1. Introduction

Within the framework of the Paris Agreement, the signing nations have agreed to keep global warming below 2 °C with respect to the pre-industrial level and to pursue efforts to limit the increase to 1.5 °C above pre-industrial levels to mitigate the effects of human caused climate change. Estimates of the remaining global carbon budget consistent with a 1.5 °C and 2 °C scenario imply that the annual global output of total emissions should be curbed down to 25 $GtCO_2e$ (carbon dioxide equivalent) and 41 $GtCO_2e$ by the year 2030, respectively (Rogelj et al., 2018). However, within the framework of current policies, the estimated annual output in 2030 will be around 60 $GtCO_2e$ and even if countries manage to reach their self-determined contributions to reduce emissions, this value will only lower to about 54 $GtCO_2e$ (Emissions Gap Report, 2019). With the remaining carbon budget rapidly diminishing, negative emission technologies (NET) are increasingly coming into focus. Instead of reducing CO_2 production, NETs focus on removing CO_2 from the atmosphere and storing it in oceanic and terrestrial sinks. Current approaches include bioenergy with carbon capture and storage (BECCS), direct air capture (DAC), Enhanced Rock Weathering (EW), afforestation, ocean fertilization and the conversion of biomass into biochar for soil amendment (Negative Emissions Technologies and

* Corresponding author.
E-mail address: Thomas.rinder@sbg.ac.at (T. Rinder).

https://doi.org/10.1016/j.jclepro.2021.128178
Received 8 January 2021; Received in revised form 28 May 2021; Accepted 29 June 2021
Available online 2 July 2021

Reliable Sequestration: A Research Agenda, 2019; Smith et al., 2016). Large scale deployment of negative emission technologies within the 21st century is an integral part of the vast majority of models, consistent with the 1.5 °C and 2 °C scenario (Workman et al., 2020). These models often imply large scale removal of atmospheric CO_2 by NETs only after 2050, allowing a temporal overshoot of our remaining carbon budget (Hilaire et al., 2019). It has been argued that within the framework of the current policies it might be impossible to reach the 1.5 °C goal without relying on negative emission technologies (Anderson et al., 2020; Hickel and Kallis, 2020). Until now different NETs are at different stages of development (Anderson and Peters, 2016), and at the moment there is no single solution for the removal of CO_2 at scale ready for deployment (Fuss et al., 2018). This has led to a more general debate whether NETs provide promising avenues for achieving the goals of the Paris Agreement (Schlesinger and Amundson, 2019). Provided the uncertainties on a global scale and with the only alternative being a more rigorous cut in emissions, it is required to precisely quantify the future potential of NETs and how they can be incorporated into climate change mitigation scenarios (Anderson and Peters, 2016; Fuss et al., 2014).

CO_2 consumption through reaction with mafic and ultramafic rocks and minerals is one of the technologies which has already been proposed 30 years ago as an industrial process (Lackner et al., 1995; Seifritz, 1990; see Kelemen et al. (2020) for an up to date review of the topic), and the potential through diffuse spreading of rock powder to the land surface has been reviewed by Schuiling and Krijgsman, (2006). This technology is referred to as Enhanced Rock Weathering (ERW), enhanced weathering (EW), or Terrestrial Enhanced Weathering (TEW). We use the term EW in this study. The concept has since been investigated in a number of different scenarios. The potential of mine tailings from mafic and ultramafic deposits has been evaluated (e.g. Assima et al., 2014, 2012; Gras et al., 2020; Hamilton et al., 2018; Harrison et al., 2013; Lechat et al., 2016; Oskierski et al., 2016; Power et al., 2020; Pronost et al., 2011; Thom et al., 2013; Wilson et al., 2014). Investigations include numerical modeling studies on global (Hartmann et al., 2013; Köhler et al., 2010; Moosdorf et al., 2014; Strefler et al., 2018; Taylor et al., 2016) and regional scale (Aviso et al., 2021; Lefebvre et al., 2019; Renforth, 2012). While some studies focus on the application to croplands (Beerling, 2017; Haque et al., 2019; Kantola et al., 2017; Taylor et al., 2017) others focus on marine environments and the effect of EW on ocean alkalinity (Bach et al., 2019; Hangx and Spiers, 2009; Montserrat et al., 2017; Renforth and Henderson, 2017; Rigopoulos et al., 2018a). Additionally, several field and lab studies have been carried out so far (Amann et al., 2020; Dietzen et al., 2018; Haque et al., 2020a, 2020b; Kelland et al., 2020; Renforth et al., 2015; ten Berge et al., 2012).

One advantage of EW is relatively low land use compared to other NETs and low use of the resource water (Smith et al., 2016). Moreover, enhanced weathering of dunite and basalt is cost competitive with respect to other methods, ranging from 60 US $ per t CO_2 for dunite to 200 US $ for basalt (Strefler et al., 2018). While the relatively high energy input required for EW related to mining, milling and transport of the rocks reduces efficiency, the CO_2 drawdown of olivine may still reach a net value of 0.5–1 t CO_2 per t of rock (Beerling et al., 2018; Moosdorf et al., 2014). Olivine is used in many studies related to EW for its high CO_2 drawdown relative to rock mass (e.g. Dietzen et al., 2018; Renforth et al., 2015, Table 1), but the potential release of toxic metals during dissolution is a disadvantage (Amann et al., 2020). In contrast, Haque and coworkers showed in a number of studies that wollastonite ($CaSiO_3$) amendment of soil is beneficial for crop yield, while at the same time increasing soil inorganic carbon content (Haque et al, 2019, 2020a, 2020b). Similarly, volcanic rock is already used for soil amelioration and results from an experimental study on the use of basalt powder, added to slightly acidic clay-loam soil, show cumulative removal of 4 t CO_2 ha^{-1} within 5 years (Kelland et al., 2020). This study also found an increasing crop yield (sorghum) by 21 ± 9.4%. In a recent study Beerling et al. (2020) indicated the potential of basalt application to cropland for CO_2 removal on a global scale. They estimated the potential of CO_2 removal for application of ground basaltic rock on cropland in the range of about 0.5–2 $GtCO_2$ y^{-1}. The aggregate amount of carbon dioxide removal, if sustained over 50 years could be between 25 and 100 Gt CO_2. The study also showed the potential for removal of CO_2 in temperate climate regions. Factors influencing the potential of EW include climate, agricultural area and practice, availability of suitable rocks, available transport networks, the CO_2 intensity of electricity generation, and CO_2 emissions from mining, comminution and transport. The importance of transport distance has been addressed by Lefebvre et al. (2019). The authors assessed the potential of basalt for EW in a part of Brazil and concluded that the maximum transport between the quarry and field would 990 ± 116 km, above which the transport related CO_2 emissions would offset the potential CO_2 capture. Therefore, if EW is to be used in the near future, the regional availability of suitable resources is a prerequisite and regionally tailored approaches are needed to put the technology to optimal use.

Here we selected Austria as suitable case example to evaluate the feasibility of EW in a regional context. Towards the realization of the European Green Deal, countries with an efficient railway network, a wide variety of lithologies within reach, and relatively high share of hydropower for electricity generation, like Austria, at first sight seem to be well suited for EW as a technology. However, before EW can be applied, it remains to be quantified whether enough suitable rocks are available in Austria or bordering countries and whether the energy demand for mining, transport and mineral comminution and consequent CO_2 production substantiate enhanced basalt weathering as a reliable strategy. In the following, we will first review the current state of research in the field before we will use our case study to demonstrate how the feasibility of EW can be evaluated in a regional setting.

Table 1
Theoretical CO_2 drawdown ($R_{CO2\ max}$ and $R_{CO2\ low}$) in kg CO_2 t^{-1} of rock (mineral) for common basalt forming minerals and basalt. $R_{CO2\ max}$ is based on congruent dissolution and $R_{CO2\ low}$ is based on incongruent dissolution. Bold numbers indicate $R_{CO2\ low}$ and $R_{CO2\ max}$ used during modeling, based on the basalt composition given in Navarre-Sitchler and Brantley (2007).

Name	Formula	g mol^{-1}	$R_{CO2\ max}$	$R_{CO2\ low}$
Forsterite	Mg_2SiO_4	140.7	1251	1251
Enstatite	$Mg_2Si_2O_6$	200.8	877	877
Diopside	$CaMgSi_2O_6$	216.5	813	813
Hornblende	$(Ca_{0.6}Na_{0.3}K_{0.1})_{2.5}(Mg_{0.6}Fe_{0.3}Al_{0.1})_5[((OH)_{0.75}F_{0.25})_2/(Si_{0.75}Al_{0.25})_2Si_6O_{22}$	868.4	811	507
Orthoclase	$KAlSi_3O_8$	278.3	632	158
Anorthite	$CaAl_2Si_2O_8$	278.2	1265	316
Leucite	$KAlSi_2O_6$	218.3	807	202
Nepheline	$Na_3KAl_4Si_4O_{16}$	584.3	1205	301
Basalt	$Si_1\ Ti_{0.025}\ Al_{0.329}\ Mg_{0.310}\ Fe(III)_{0.02}\ Fe(II)_{0.193}\ Ca_{0.273}\ Na_{0.061}\ K_{0.007}\ O_{3.394}$	123.5	968	429
Basalt	$Ca_{0.3}Mg_{0.1}Fe_{0.4}Al_{0.3}SiO_{3.25}$	125.0	**880**	**282**

2. Theoretical background and methodology

2.1. Rock powder for soil amelioration

One of the goals proclaimed in the Paris agreement on climate change is to "[…] foster climate resilience and low greenhouse gas emissions development, in a manner that does not threaten food production". In this context, the potential co-benefits of soil amelioration through application of basaltic rocks to croplands are noteworthy. They largely contrast the societal friction points, related to competition for land use, connected to BECCS, afforestation and reforestation. In addition, EW could be co-deployed for the two latter technologies (Amann and Hartmann, 2019; Kantola et al., 2017). Application of silicate –rock fertilizers to agricultural land is not a new concept and it has been investigated already by e.g. Hensel (1894) or more recently by e.g. Van Straaten (2006). The potential benefits are linked to the fact that silicon is actively accumulated in a number of crops including wheat, barley and sugar beet (Guntzer et al., 2012). Benefits of silicon accumulation are especially important under environmental stress because silicon alleviates toxicity of some toxic metals, improves Potassium, Phosphor and calcium uptake, alleviates the effects of drought and increases resistance to pathogens and insects (Adrees et al., 2015; Guntzer et al., 2012). The recycling of plant silicon in unaltered ecosystems accounts for a high percentage in the silicon pool, owed to the re-dissolution of plant phytoliths. Under agricultural use, however, this cycle is interrupted due to the removal of crops. Especially with silicon accumulating plants this can warrant silicon fertilization (Savant et al., 1997), and a positive effect on yield has been reported for instance in the case of wheat with a grain yield increase of 4.1–9.3% (Liang et al., 1994). Soil amendment through application of basalt has positive effects on the cation exchange capacity in soils and supplies potassium, phosphor and calcium (Gillman et al., 2002). In addition aluminum toxicity is a problem with acid soil conditions around the world. Silicon in general and basalt in particular have been shown to effectively decrease aluminum toxicity in acid soils (; Cocker et al., 1998; Shamshuddin and Kapok, 2010). For these potential co-benefits, basaltic rock may be the best candidate for EW through application on agricultural land, despite its relatively low capability to sequester CO_2, compared to dunite. Moreover release of Chromium, Nickel and Cobalt from dunite (Renforth et al., 2015; ten Berge et al., 2012) and serpentinites (Kierczak et al., 2016) and potential accumulation in soil and crops may counteract the intended soil amelioration and the same is true for low Ca/Mg ratios (Echevarria, 2018). While serpentinites and amphiboles might exhibit good reactivity, asbestos group minerals are generally a safety concern during mining, milling, and spreading of rock powder, thereby even if handled in a safe way, public perception could impose barriers on their application (Gwenzi, 2020).

2.2. CO_2 drawdown through weathering

Over geological time scales, atmospheric carbon dioxide is affected by the weathering of silicate rocks through the transformation of CO_2 into HCO_3^- (Amiotte Suchet et al., 2003; Berner et al., 1983; Dessert et al., 2003; Gaillardet et al., 1999; Gislason et al., 2009; Walker et al., 1981). For instance, the rise of the Himalayas and consequent increased weathering has resulted in CO_2 drawdown and a general cooling of global climate (Raymo and Ruddiman, 1992). Similarly, past cooling phases of the climate since the Archean could be directly linked to the drawdown of CO_2 from the atmosphere (e.g. Elliot Smith et al., 2008; Kump et al., 1999; Lowe and Tice, 2004). The idea behind EW is to speed up this process through grinding of rocks and targeted application to increase weathering rates. Exemplarily the chemical reaction can be followed through incongruent dissolution of anorthite (eq. (1)). The dissolution of primary silicates leads to formation of secondary precipitates, releasing cations and transforming CO_2 into HCO_3^-.

$$CaAl_2Si_2O_8 + 2CO_2 + 3H_2O \rightarrow Al_2Si_2O_5(OH)_4 + Ca^{2+} + 2HCO_3^- \quad (1)$$

Ideally the HCO_3^- ion will subsequently be transported to the ocean (Renforth and Henderson, 2017), where it possibly partially alleviates ocean acidification (Hartmann et al., 2013; Taylor et al., 2016). If supersaturation with respect to individual carbonate phases is reached, solid carbonates might form (eq. (2)).

$$Ca^{2+} + 2HCO_3^- \rightarrow CaCO_3 + CO_2 + H_2O \quad (2)$$

Carbonate formation is an important mechanism for the in situ fixation of CO_2 through Carbon Capture and Storage (For a review of mineral carbonation in general see e.g. Kelemen et al., 2020; Snæbjörnsdóttir et al., 2020). However, the aim of enhanced weathering is to convert CO_2 into alkalinity, as the formation of carbonates will reduce the processes efficiency (eq. (2)).

The maximum amount of CO_2 drawn from the atmosphere through silicate dissolution is a function of the cation flux (mostly Ca^{2+}, Mg^{2+}, K^+ and Na^+) which is charge balanced by the formation of HCO_3^-. Drawdown potential can be expressed as the amount of CO_2 (R_{CO2}) removed from the atmosphere per mass of rock (t CO_2 t^{-1} of rock). This value might be reduced during riverine transport (Hotchkiss et al., 2015; Marx et al., 2017; Polsenaere et al., 2013) and it will further decrease, depending on the apparent carbonate equilibrium in the ocean (Beerling et al., 2020). For the relatively fast weathering of Ca and Mg bearing silicates, R_{CO2} is sometimes based solely on Mg^{2+} and Ca^{2+} contents (Renforth, 2012). In the case of basalt the contribution of monovalent cations (Na^+ and K^+) needs to be included, as they are frequently present in mafic and ultramafic volcanic rocks (see Table 1) in the form of relatively fast weathering minerals such as nepheline (Tole et al., 1986). In addition, the calculation of R_{CO2} from incongruent dissolution, is based on the idea of aluminum conservation through the formation of secondary minerals (eq. (1)). However, congruent dissolution of the aluminosilicate will precede the formation of the secondary phase (Maher et al., 2009; Steefel and Van Cappellen, 1990) (eq. (3)), and far from equilibrium conditions can be sustained during basalt weathering for instance through complexation of Al^{3+} with organic acids (Perez-Fodich and Derry, 2019).

$$CaAl_2Si_2O_8 + 8CO_2 + 4H_2O \rightarrow 2Al^{3+} + Ca^{2+} + 8HCO_3^- + 2SiO_{2(aq)} \quad (3)$$

Table 1 provides the R_{CO2} for minerals commonly found in basalt and two different compositions of basalt (Gudbrandsson et al., 2011; Navarre-Sitchler and Brantley, 2007). $R_{CO2\ low}$ is based on incongruent dissolution, where CO_2 is charge balanced against the cations released during dissolution ($\Sigma CO_2 = meq(Ca^{2+} + Mg^{2+} + Na^+ + K^+)$). $R_{CO2\ max}$ is based on congruent dissolution including Al^{3+}, Fe^{3+}, Fe^{2+} and Ti^{4+} in the calculation. The latter process has also been proposed in (Navarre-Sitchler and Brantley, 2007) to asses CO_2 drawdown from basalt weathering. The values of 282 kg t^{-1} of basalt ($R_{CO2\ low}$) and 880 kg t^{-1} of basalt ($R_{CO2\ max}$) will be used for evaluation of the potential in a pessimistic and optimistic scenario in this study.

2.3. Basalt weathering rates in the context of enhanced weathering

The dissolution of basaltic glass at far from equilibrium conditions has been investigated in mixed flow reactors by (Galeczka et al., 2014; Gislason and Oelkers, 2003; Oelkers and Gislason, 2001; Stockmann et al., 2011; Wolff-Boenisch et al., 2004). These studies show a minimum dissolution rate in the circumneutral pH area (see Fig. 1), commonly observed for aluminosilicates (Gautier et al., 1994; Gudbrandsson et al., 2014). In contrast, Al-free silicate minerals, such as enstatite or forsterite exhibit a near linear dependence of dissolution rates on pH (Fig. 1). Accordingly, the respective mineralogical composition of a basaltic rock may influence the stoichiometry of the released cations. This has been shown in experiments, where a U-shaped release of Ca^{2+} as a function of pH was shown, connected to the dissolution of plagioclase, while for

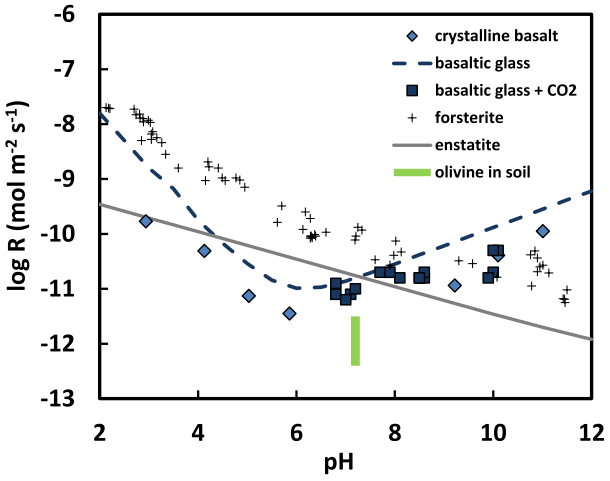

Fig. 1. BET normalized dissolution rate of basalt, forsterite and enstatite (based on Silica release) as a function of pH at 25 °C. Crystalline basalt (Gudbrandsson et al., 2011), basaltic glass calculated from (Gislason and Oelkers, 2003), basaltic glass + CO_2 (Stockmann et al., 2011), forsterite (Pokrovsky and Schott, 2000), enstatite (Oelkers and Schott, 2001) and olivine, added to soil (Renforth et al., 2015).

Mg^{2+} and Fe^{2+}dominantly released from pyroxenes and olivine a linear decrease was observed (Gudbrandsson et al., 2011). The reactivity of basalt was not hindered by the formation of secondary carbonates in the experiments carried out by Stockmann (2011). Basaltic glass and its crystalline counterparts exhibit a similar pH dependence on dissolution rates, which decrease with increasing Silicon content of the solid phase. Wolff-Boenisch et al. (2006) investigated the influence on crystallinity on dissolution rates of silicate minerals and their amorphous counterparts at pH 4 and found that crystallinity influences the dissolution rate for Silicon rich phases, whereas ultramafic glasses dissolve similar to their crystalline counterparts. In general, dissolution rates of volcanic rocks decrease with increasing Silicon content (Wolff-Boenisch et al., 2004).

To understand better the importance of mafic and ultramafic rocks as reactants in the long term global Silicon Carbon cycle, basalt weathering rates have been estimated at catchment scale in several studies (e.g. Babechuk et al., 2014; Das et al., 2005; Dessert et al., 2001; Li et al., 2016; Louvat and Allègre, 1997; Moulton et al., 2000). However, reconciling the observations from field scale with the laboratory derived weathering rates remains a challenge. In general the difference in laboratory and field rates can be attributed to both, physical i.e. hydrological features (Velbel, 1993), chemical features such as surface passivation though leached layer formation or the precipitation of secondary phases (Daval et al., 2018; Velbel, 2009), or a mixture of both, such as a long fluid residence times. The prediction of surface passivation itself is not straightforward. For instance the formation of passivating layers may be prevented through fungal biofilm, thereby increasing dissolution rates (Gerrits et al., 2020). On the other hand, the passivating effect of Al on the solubility and dissolution rate of amorphous silica and quartz has been investigated by (Bickmore et al., 2006; Iler, 1973), showing that Al containing layers not only reduce dissolution rates but also apparent overall solubility. Fluid residence time, soil moisture and mineral/fluid ratios are crucial when investigating the rate of chemical weathering (Maher, 2010; Navarre-Sitchler et al., 2011; White and Brantley, 2003). The complex interrelationship between gas and water in the unsaturated zone further complicates the calculation of realistic weathering rates (Harrison et al, 2015, 2017). In addition, field weathering rates are influenced by trace metals (Oelkers et al., 2018), bacterial communities (Wild et al., 2019) or organic ligands (Perez-Fodich and Derry, 2019; Perez et al., 2015). They are not only dependent on a specific surface area but can be influenced by crystallographic orientation of minerals (Daval et al., 2013).

In the context of enhanced weathering, dissolution of rock powder added to soil cannot be calculated merely based on dissolution rates. The shrinking core model has been used to describe the time for complete dissolution of a grain (Hangx and Spiers, 2009). The authors estimated that the addition of olivine to seawater requires particle sizes <10 μm to achieve relatively complete dissolution of 100 years. With a similar approach Renforth et al. (2015) estimated that the particle size of olivine added to soil, would have to be in the range of 0.1–0.01 μm to dissolve within 5 years.

Notwithstanding the uncertainties related to field weathering, in this study dissolution was calculated, using a dissolution rate from (Gudbrandsson et al., 2011), who measured a BET surface (Brunauer et al., 1938) normalized rate of 3.55 10^{-12} mol m^{-2} s^{-1} at pH 5.84 and 25 °C (see Fig. 1). This is probably at the high end of weathering rates, given the discrepancy between lab and field rates and 25 °C is certainly far away from the annual average temperature in Austria. It is however close to the high end of dissolution rates reported for olivine in soil (Renforth et al., 2015) (see Fig. 1), and it is also in the range of the elemental release rates reported for basalt added to soil (Kelland et al., 2020). These authors measured an elemental Mg release rate of 6.6 10^{-13} mol m^{-2} s^{-1} and a Ca release of 2.8 10^{-12} mol m^{-2} s^{-1}. For comparison, the stoichiometric dissolution of our model basalt (Table 1) at the chosen rate gives an elemental release rate for Mg of 3.54 10^{-13} mol m^{-2} s^{-1} and 1.06 10^{-12} mol m^{-2} s^{-1} for Ca.

The BET surface area of the model basalt was calculated using an empirical equation, provided in (Brantley and Mellott, 2000) for olivine, where d is the particle diameter.

$$\log SSA\ \left(cm^2 g^{-1}\right) = 5.3 - 1.1 * \log(d) \quad (4)$$

Molecular weight of the basalt is 125 $gmol^{-1}$ and the assumed density is 3 g cm^{-3}.

2.4. A modified shrinking core model

The shrinking core model (Hangx and Spiers, 2009) assumes spherical grains to model the dissolution process, which accordingly only approximates surface-volume ratios of natural grains. For this reason a steady state model, i.e. a scenario in which the specific surface area does not change over time, has been used in Strefler et al. (2018). To circumvent potential shortcomings of both approaches we include the roughness ratio (SSA_{BET}/SSA_{Geo}) into the shrinking core model, where SSA_{BET} refers to the specific surface area calculated from gas adsorption according to Brunauer et al. (1938) and SSA_{GEO} refers to the specific surface area, based on spherical particles according to the equation provided in (Tester et al., 1994). BET normalized dissolution rates are recalculated to the geometric surface area of spherical grains of each fraction (see the supplementary file for details about the calculation). This way the overestimation of the amount of dissolution (steady state) as well as underestimation (applying BET normalized dissolution rates to a shrinking core model) can be avoided (see Fig. 4 and discussion).

2.5. Geographical framework and model parameters

2.5.1. Availability of volcanic rocks in Austria and neighboring countries

Potential occurrences of volcanic rocks in the vicinity of Austria comprise units from the Western and Central European volcanic province in the Massif Central (Lustrino and Wilson, 2007), the Bohemian Massif and Eger Graben (Ulrych et al., 2011), Germany (Jung et al., 2005; Jung and Masberg, 1998), the Pannonian-Carpathian Volcanic province – parts of which are based in SE Austria (Ali et al., 2013; Downes et al., 1995; Lukács et al., 2018; Seghedi et al., 2004) and the Veneto Volcanic province in Northern Italy (Peccerillo, 2005) as well as some occurrences in the Dinaric alps (Prelević et al., 2005), (see Fig. 2).

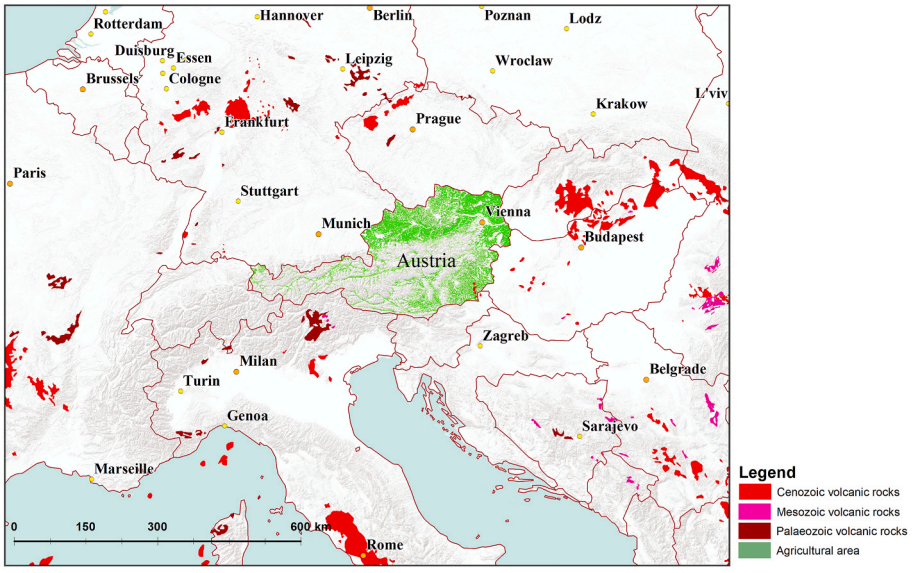

Fig. 2. Map showing the distribution of agricultural land in Austria and potential volcanic rocks in the wider vicinity. Layers: World terrain basemap (Sources: Esri, USGS, NOAA); World cities (Sources: Esri; Bartholemew and Times Books; U.S. Central Intelligence Agency (The World Factbook); International Organization for Standardization; United States Department of State, Bureau of Intelligence and Research; GeoNames; Executive Secretary for Foreign Names - U.S. Board on Geographic Names; U.S. National Geospatial-Intelligence Agency; BBC News; Global Mapping International); CORINE land cover 2018 (© Umweltbundesamt & European Union, Copernicus Land Monitoring Service 2018, European Environment Agency (EEA), with funding by the European Union); © EuroGeographics for the administrative boundaries; volcanic rocks from IGME-5000 (Asch, 2005). The map was created using ArcGIS® software by Esri. ArcGIS® and ArcMap™ are the intellectual property of Esri and are used herein under license. Copyright © Esri. All rights reserved.

Relatively large volcanic provinces of Permo-Carboniferous origin appear south of the Insubric line, mostly comprising intermediate to felsic volcanic rocks, e.g. dacite, trachyte, rhyolite (Cortesogno et al., 1998). The same is true for relatively large volcanic fields close in the West Carpathians, such as the central Slovakian volcanic field, mostly comprising andesite (Chernyshev et al., 2013). Similarly, volcanic rocks of the roman volcanic province are largely of intermediate composition (Beccaluva et al., 1991). (Plata et al., 2021) investigated the potential of andesitic and dacitic mining waste as a soil fertilizer, showing that soil amelioration is not limited to volcanic rocks with a low Silica content. However, Cenozoic volcanic rocks of ultramafic to mafic composition can be found in all volcanic provinces surrounding Austria (see Fig. 3). The impression gained from Fig. 3 also holds when compared to the more extensive database of volcanic rocks provided in (Lustrino and Wilson, 2007), or with respect to the data provided by (Hartmann and Moosdorf, 2012), who calculated the percentage for basic volcanic rocks of ≈59.5%, with intermediate compositions contributing 8.5% and acid compositions covering an area of 32% for whole Europe. However, for Central Europe, basalt may not be main rock source and other mafic volcanic rocks such as basanite or trachybasalt might need to be included to provide the enormous amounts of rock required. As noted above, differences in mineralogical and chemical composition are both crucial for the value as a fertilizer as well as dissolution kinetics. Accordingly, when we refer to basalt in this manuscript it should be considered as representative for a range of ultramafic and mafic volcanic rocks, which warrant closer examination in the future.

2.5.2. *Agricultural areas in Austria*

Cropland area covered approximately 1.325 M ha in 2019 (Statistik Austria, 2020), and additional 0.576 M ha were categorized as intensive grassland (Statistik Austria, 2018), assumed to be easily available for inorganic fertilizer application. Out of 1152 representative soil samples 38% have a soil pH > 7, in 53% of samples the pH ranges from 5 to 7 and 9% are characterized as strongly acidic (pH = 4–5). For grass land only 6% show a pH > 7. The pH of 55% of the samples falls in the range of 5–7, and 39% of the samples are between pH 4 and pH 5 (Schwarz and Freudenschuss, 2004). Soil amelioration is mostly proposed for acidic soils. However, from a perspective of CO_2 sequestration, soil pH has relatively low impact as long as basalt is used. The dissolution rate of basaltic glass in the relevant range (4–8.5) reaches a minimum around pH 6 (see Fig. 1). Compared to this minimum, dissolution rate is ≈ 3 times faster at pH 5 and also ≈3 times faster at pH 8. A pronounced pH effect would only be expected for very acid conditions – at pH 4 the dissolution rate is ≈ 17 times that of pH 6 (Gislason and Oelkers, 2003). From this perspective basaltic soil amelioration could also be applied to lime rich alkaline soils, where it could provide a potassium source, decreasing the need for conventional fertilizers. In summary, an area of 1.902 M ha (cropland plus intensive grassland) are assumed to be a reasonable maximum area of application and will be used in further modeling exercises.

2.5.3. *Mining, transport and comminution*

The energy demand related to crushing and grinding of material in order to reach particle sizes small enough to achieve desirable weathering rates in soil are considered and important drawback of EW (Gerdemann et al., 2007; Moosdorf et al., 2014; Renforth et al., 2015; Rigopoulos et al., 2018b). To evaluate the interrelationship between CO_2 emissions from comminution and drawdown rate of CO_2, three scenarios with different grain size distribution are used for modeling. The selected particle size distribution ranges from 100 to 0.1 μm (<100 μm), 10–0.1 μm (<10 μm) and 1–0.1 μm (<1 μm). The particle size distribution was calculated for fixed classes, with normal distribution with a μ of 50, 5 and 0.5 and σ of 30, 3 and 0.3, respectively. The resulting grain size distribution can be found in the supplementary file (Table S1). Comminution, mining and application can be considered static and resulting input parameters used for calculation of the CO_2 balance are listed in Table 2. Based on the relatively widespread availability of mafic and ultramafic volcanic rocks (see above) the average distance from mine to field was estimated about 300 km. This is an optimistic approach, assuming that the quarries closest to the Austrian border are also able to produce the required amount and quality. Resulting transport related CO_2 emissions considered in this study, are 4.8 kg CO_{2e} t^{-1}, 18.9 kg CO_{2e} t^{-1} and 59.4 kg CO_{2e} t^{-1}, for transport by rail, a <7.5 ton truck and 20–40 ton truck, respectively. Total CO_{2e} emissions including mining, comminution, transport and application calculated on base of 300 km transport are shown in Table 3 for three scenarios, using different grain size distributions (<100 μm, <10 μm, <1 μm).

3. Results and discussion

3.1. *Assessment of the modified shrinking core model*

Strefler et al. (2018) used a steady state model to estimate the dissolution of rock powder. Such a model assumes that dissolving powder is always present in the same amount and accordingly the

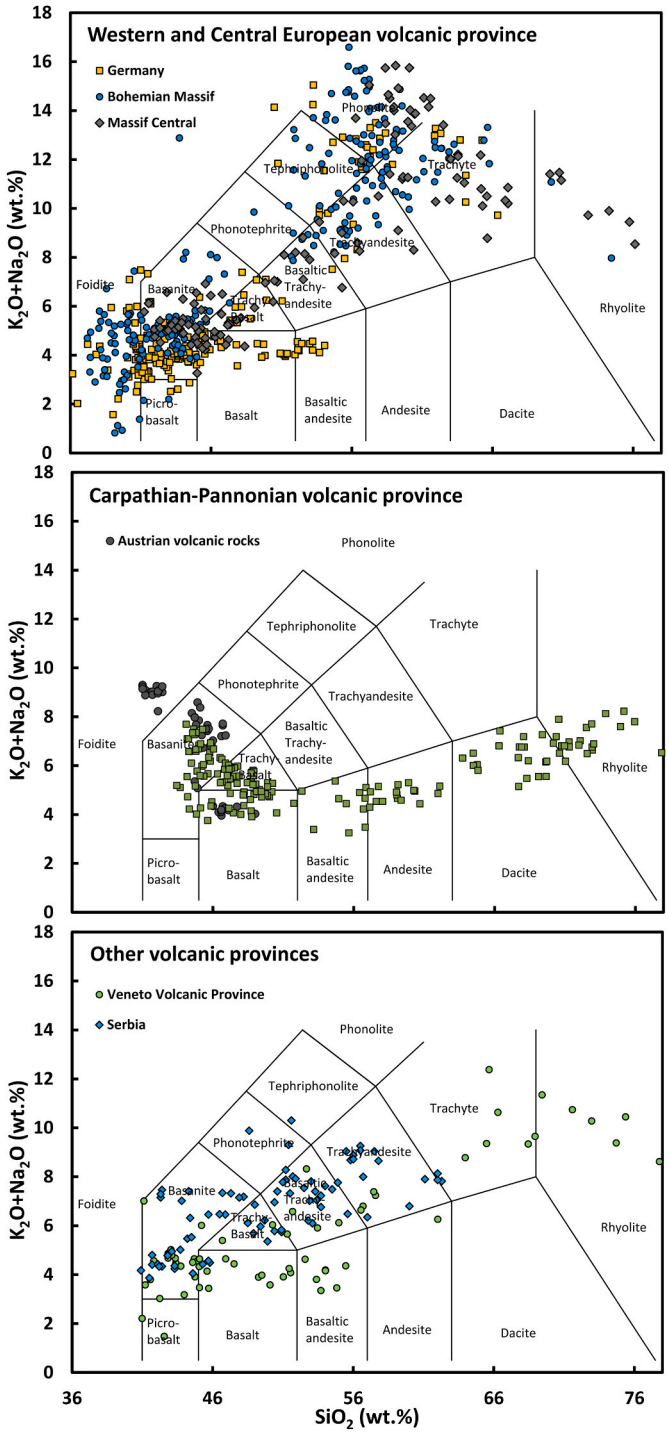

Fig. 3. Total alkali content (Na_2O + Na_2O) versus Si_2O of selected volcanic rocks in the wider vicinity of Austria. (a) Carpathian – Pannonian region; data from (Ali et al., 2013; Ali and Ntaflos, 2011; Harangi et al, 2007, 2015, 2007; Lukács et al., 2018), (b) Western and Central European volcanic province (Alibert et al., 1983; Briot et al., 1991; Chauvel and Jahn, 1984; Dautria et al., 2004; Haase et al, 2004, 2017, 2004; Hegner et al., 1995; Jung et al., 2006; Jung and Masberg, 1998; Mertes and Schmincke, 1985; Riley et al., 1999; Ulrych et al, 2003, 2011, 2003; Wilson et al., 1995; Wörner and Schmincke, 1984); (c) Other volcanic regions (Macera et al., 2003; Milani et al., 1999; Prelević et al., 2005).

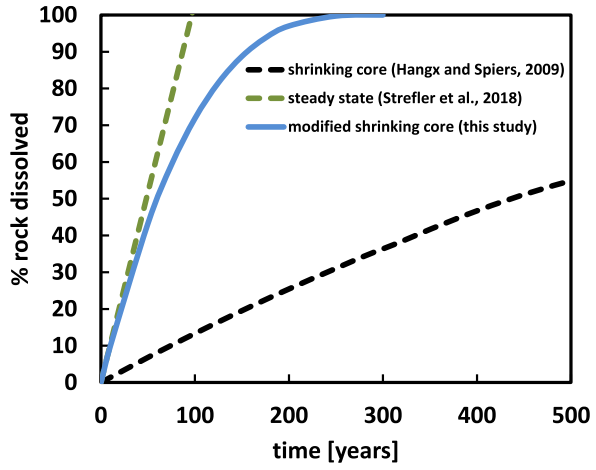

Fig. 4. Dissolution of basalt powder with a grain size of 20 μm and an of SSA_{BET} of 0.74 $m^2\ g^{-1}$ at a rate of 3.55 10–12 mol $m^{-2}\ s^{-1}$ calculated after Hangx and Spears (2009), Strefler et al. (2018) and this study.

Table 2
Input parameters, used for the calculation of the CO_2 balance.

	kg CO_2 kWh^{-1}	kg CO_2e t^{-1} km	kWh t^{-1}	kg CO_2 t^{-1}
electricity generation (Austria)[a]	0.26			
Road transport (<7.5 t)[b]		0.198		
Road transport (20–40 t)[b]		0.063		
Railway transport[b]		0.016		
comminution (<100 μm)[c]			18.9	4.9
comminution (<10 μm)[d]			173.0	45.0
comminution (<1 μm)[e]			556.0	144.6
Mining[e]				7.0
application low estimate[e]				1.0
application high estimate[e]				4.0

[a] https://secure.umweltbundesamt.at/co2mon/co2mon.html.
[b] (Schmied and Knörr, 2013).
[c] Energy requirement for comminution to <100 μm from the table of bond work index (https://www.911metallurgist.com/blog/table-of-bond-work-index-by-minerals).
[d] (Hangx and Spiers, 2009).
[e] (Moosdorf et al., 2014).

Table 3
Total CO_2 emissions in kg t^{-1} of rock, including mining, transport (300 km), comminution and application.

Grain size	Railway transport	Road transport (20–40 t)	Road transport (<7.5 t)
<100 μm	17.7	31.8	75.3
<10 μm	57.8	71.9	115.4
<1 μm	157.4	171.5	215.0

surface area available for water rock interaction does not change over time. They used a 20 μm powder with a SSA_{BET} of 1.69 $m^2\ g^{-1}$ and yielded a dissolution of 19.6% within 1 year. In general our scenario is relatively conservative compared to that. With a SSA_{BET} of 0.74 $m^2\ g^{-1}$ and a lower dissolution rate of 3.55 10^{-12} mol $m^{-2}\ s^{-1}$ the steady state model would result in only 1.03% of the powder dissolved within 1 year. Interestingly, using our modified shrinking core model, we calculate a similar amount of 1.03%. Apparently, accounting for the shrinking core is not very important during initial stages of dissolution and a steady state approach seems valid even with the 19.6% dissolved in Strefler

et al. (2018) (see Fig. 4). However, as the dissolution of the basalt powder continues over several years, a steady state model becomes increasingly unrealistic. The complete dissolution according steady state assumption takes 97 years, in which case only 70% of the powder are dissolved using our modified shrinking core (see Fig. 4). The shrinking core as originally proposed in Hangx and Spiers (2009) dissolves only 0.14% of powder within 1 year and the complete dissolution takes 2120 years. This underestimation is however a result of applying a BET normalized dissolution rate to the geometric surface of a sphere and simple recalculation can circumvent this problem (see supplementary file for details). Accordingly, we propose the shrinking core model applied in this study as a plausible way to estimate the dissolution of rock powder.

3.2. Influence of particle size on weathering rates

Based on Eq. (4) the average SSA_{BET} resulting is 10.53 (<100 μm), 18.61 (<10 μm) and 67.42 $m^2\ g^{-1}$ (<1 μm), respectively. Time for complete dissolution of the powder was calculated to be 1696, 134 and 10.7 years for the <100 μm, <10 μm and <1 μm powder, respectively. However, as the reservoir gets depleted and the grains become increasingly small, dissolution becomes relatively ineffective and for instance 87% of a 100 μm grain will have dissolved in half the time, needed for complete dissolution. Accordingly, the evaluated timeframe in Table S1 and Fig. 5 is for 97.5% dissolution in which case the dissolution takes 1205, 96 and 7.6 years. As this time is based on the largest size grains in each powder, smaller grains will dissolve completely and based on the chosen grain size distribution >99.9% of the basalt powder will dissolve within the chosen timeframe (see Fig. S1 in the supplementary file).

The potential CO_2 drawdown associated with the dissolution of the respective powder is shown in Fig. 5a–c for the first 10 years and $R_{CO2\ max}$ and $R_{CO2\ low}$. Based on their experiments, Kelland et al. (2020) modeled a cumulative removal of CO_2 of 44 kg $CO_2\ t^{-1}$ of basalt within 5 years through the application of basalt with a diameter of <128 μm in good agreement with our calculation for the <100 μm (Fig. 5a) which yields a drawdown 35 kg $CO_2\ t^{-1}$ after 5 years. Within the chosen observation period, increasing the reaction rate through decreasing the grain size is decisive in the $R_{CO2\ low}$ and the $R_{CO2\ max}$ scenario (see Fig. 6). Apparently comminution, despite its high energy demand is not the controlling factor on the CO_2 drawdown. On the contrary, given the slow dissolution of the <100 μm fraction (1698 years for complete dissolution), even best practice (rail transport) will only contribute limited to climate change mitigation (see Table S2 and Fig. 6), and in the case of poor logistics (truck transport <7.5 t) it could take ≈ 40 years until the CO_2 balance reaches at least net 0. However, under a $R_{CO2\ max}$ scenario, considerable CO_2 drawdown could be reached even with a relatively large particle size. It can be argued that $R_{CO2\ max}$ is high and has not been proposed by any of the other studies in context with basalt application. The exact mechanisms of CO_2 drawdown during basalt weathering and the corresponding $R_{CO2\ max}$ are still unclear (see above) but in any case the assumed drawdown is close to the drawdown for e.g. olivine, showing the potential within ultramafic rocks in general. We note that grinding down to <1 μm is to our knowledge technically not possible at this moment at industrial scale. Notwithstanding the practical implications of the high energy demand (see section 3.3) it goes to show however that the smallest technically possible grain size should be aimed at.

3.3. Cumulative CO_2 removal in Austria

Assuming the maximum application on both intensive grassland (0.576 M ha) and agricultural land (1.326 M ha), we estimate the amount of CO_2 drawdown potential for the application of 10 kg rock m^{-2} (100 t ha^{-1}). The cumulative amount of basalt applied in this case is 190 Mt. Using rail transport and $R_{CO2\ low}$, this amounts to a removal of

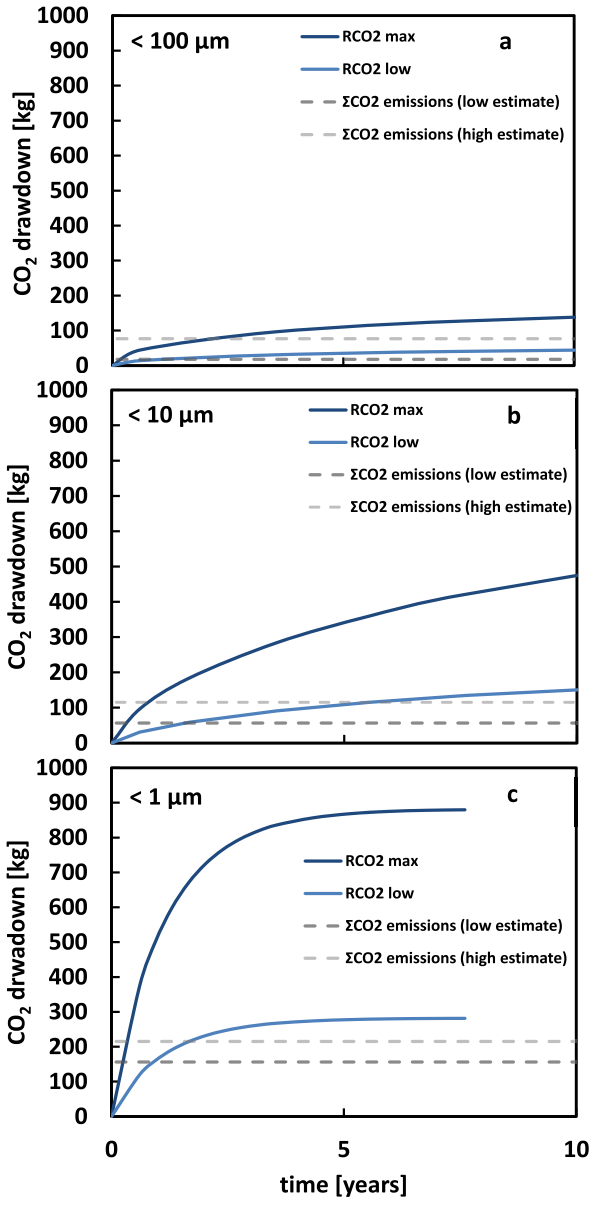

Fig. 5. Evolution of CO_2 drawdown in kg t^{-1} of basalt, using $R_{CO2\ low}$ of 282 kg and $R_{CO2\ max}$ of 880 kg. Grey dashed lines denote the estimates for CO2 emissions, generated through mining, grinding, transport (300 km) and application; the low estimate is based on railway transport; the high estimate is based on road transport using a <7.5t truck.

5.2 and 18.3 Mt CO_2 for the <100 and <10 μm fraction, respectively. The annual output of greenhouse gases in Austria amounts to roughly 80 Mt CO_2e (Klimaschutzbericht, 2019). This translates to a net removal of 6.5% and 22.9% of Austria's annual greenhouse gas emissions (CO_2e) within a 10 year cycle (see Table S2). It is important to note however, that current transportation practices could easily turn this into a positive emission technology (see Fig. 6a and Table S2). For R_{CO2max} the potential drawdown would be tremendous from 29.2% (<100 μm) up to a maximum of 100.5% (<10 μm) of Austria's annual greenhouse gas emissions (CO_2e) within a 10 year cycle. This is in good agreement with the study of (Moosdorf et al., 2014), who used a comparable R_{CO2} to evaluate the potential of ultramafic rocks and found that on a global scale transport would not influence CO_2 drawdown in a way which makes the application unfeasible. We note however that including reaction rates, the gross CO_2 removal after 10 years in our estimate is 140

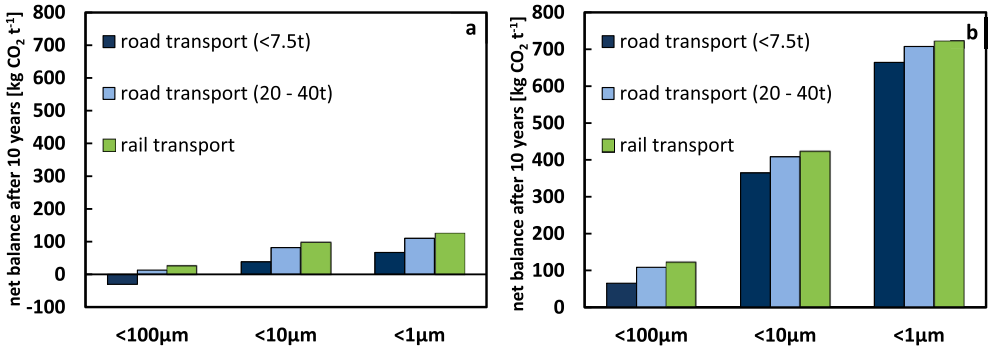

Fig. 6. CO_2 balance after 10 years for different scenarios (see Table S2), and $R_{CO2\ low}$ of 282 kg CO_2 t^{-1} rock (a) and $R_{CO2\ max}$ of 880 kg CO_2 t^{-1} rock (b).

(<100 µm) and 480 (<10 µm) kg CO_2 t^{-1}. The range of 500–1000 kg CO_2 t^{-1} obtained for complete dissolution is misleading because it hides the timeframe needed to achieve such drawdown.

3.4. A global perspective on the cumulative CO_2 removal

In a previous study Strefler et al. (2018) considered a global area of 7.9 M km^2 for application of rock powder (15 kg m^{-2}), and estimated a drawdown of 4.9 Gt CO_2 a^{-1}. We note that the dissolution rate underlying this estimate is an order of magnitude higher than ours. Using the modified shrinking core model, 6.3% of the <100 µm powder dissolve within one year, compared to 19.6% in Strefler et al. (2018). The catchment conversion equation provided by those authors yields a drawdown of 1.65 Gt CO_2 a^{-1}. This number increases to 4.0 Gt CO_2 a^{-1} for powders with grain size <10 µm, and to 15.4 Gt CO_2 a^{-1} for powders with grain size <1 µm, respectively. These numbers however refer to the gross CO_2 drawdown. Including the emissions from the 300 km railway scenario, mining, comminution and application the drawdown roughly balances the emissions during the first year (see Fig. 7). Accordingly, the actual net drawdown is much lower. After 10 years 16% of the powder (<100 µm) is dissolved. As a result the cumulative net CO_2 drawdown after 10 years will only be 2.54 Gt, i.e. 0.254 Gt CO_2 a^{-1}. If applied annually over the course of 10 years, the CO_2 drawdown increases from approximately zero in the first year to a cumulative removal of 3.2 Gt CO_2 a^{-1} in year 10. The annual application on a global area of 7.9 M km^2 at the suggested rate of 15 kg m^{-2} sums up to 118.5 Gt, and this amount would have to be added every year in order to reach the cumulative 3.2 Gt CO_2 a^{-1}. The large volume of rock needed in this scenario is in conflict with the relatively low annual application rate of 3 Gt a^{-1} of basalt to sequester 1 Gt CO2 a^{-1}, proposed in Strefler et al. (2018). But, other than suggested through a steady state model, it is not possible to simply replenish the amount of dissolved powder, considering how weathering differs depending on grain size. Smaller grains dissolve first, as the larger ones stay, which do not offer as much exposed surface.

A recent estimate applied 5.9 Gt of rock per year to reach the goal of 1 Gt CO_2 a^{-1} using a powder with grain size of <100 µm (Beerling et al., 2020). The reactive transport model in this study contains a range of parameters such as soil pH or biological impacts that are not considered in our assessment. Nevertheless it is possible to compare the two approaches. At our given R_{CO2} of 0.282 t CO_2 t^{-1} of rock, reaching a drawdown of 1 Gt CO_2/5.9 Gt of basalt requires that 59% of the basalt dissolve. Within the timeframe of 10 years the respective dissolution is 16% (<100 µm). To achieve the required drawdown with the modified shrinking core model we would have to apply a dissolution rate of basalt of 5.5 10^{-11} mol m^{-2} s^{-1}, which is close to the dissolution rate of basalt under acidic conditions at pH 4 and 25 °C (see Fig. 1). With the respective chosen dissolution rate and including emissions from the 300 km railway scenario the annual reapplication of powder reaches a removal of 0.16 Gt CO_2 a^{-1} (<100 µm) after 10 years (see Fig. S2). Averaged over the timeframe of 10 years the drawdown is only 0.08 Gt CO_2 a^{-1} (<100 µm). Using a powder (<10 µm) the dissolution after 10 years is 54% and the annual reapplication amounts to 0.57 Gt CO_2 a^{-1} with an average of 0.24 Gt CO_2 a^{-1}. The extent to which this accumulation effect is valid is governed by a range of criteria, including surface passivation of grains.

The relationship between grain size dependent weathering and transport related emissions is shown in Fig. 7. For truck transport the offsetting distances, at which potential carbon capture (R_{CO2min} of 0,282 t CO_2 t^{-1} of rock) is neutralized by transport related emissions, increase from approximately 630 km (<1 µm) to 1340 km (<100 µm). This is in good agreement with the estimates from Lefebvre et al. (2019) who calculated an offsetting distance around 990 km for enhanced weathering. But relating transport emissions to potential carbon capture does not account for the time needed to dissolve the basalt powder. Considering the drawdown after 10 years this distance decreases to 160 km (<100 µm), but it stays 630 km using the fine powder (<1 µm), which will dissolve almost completely within 10 years. Using railway transport, offsetting distances, related to potential carbon capture, decrease from 16,800 km (<100 µm) to 8000 km (<1 µm). Considering the drawdown after 10 years the offsetting distance of the <100 µm powder is still 2000 km and it stays at 8000 km for the fine powder (<1 µm).

These calculations show that it may be possible to accept larger transport distances for very fine particles, despite the high energy demand for grinding. In contrast, the use of quarry fines with a size <5 mm was evaluated by Lefebvre et al. (2019). The dissolution of a 5 mm grain according to our shrinking core model takes around 120,000 years. Not knowing the actual grain size distribution of the quarry fines, we can still hypothesize that they will be very unlikely to contribute to CO_2 drawdown within a reasonable timeframe, independent of the actual transport distance.

3.5. Energy requirement

The electricity generation in Austria amounted up to 73,460 GWh in the year 2019, and 20,901 GWh of that was generated through biogenic or fossil fuels (https://www.e-control.at/betriebsstatistik2019). For grinding down of 190 Mt of basalt to <10 µm and <100 µm, 32,904 GWh and 3595 GWh are needed, respectively. This is approximately 45%–4.9% of the annual power generation. Given the relatively long time for complete dissolution of the powder, it can be argued, that application would not be carried out every year and the optimal application rate is yet to be determined. Still, even if the application cycle is 10 years the energy requirement is 4.5% (<10 µm) or 0.5% (<100 µm) of annual electricity generation. A detailed analysis of the transformation and growth potential of the energy sector in Austria over the next decades is outside the scope of this study. However we note, that back until the

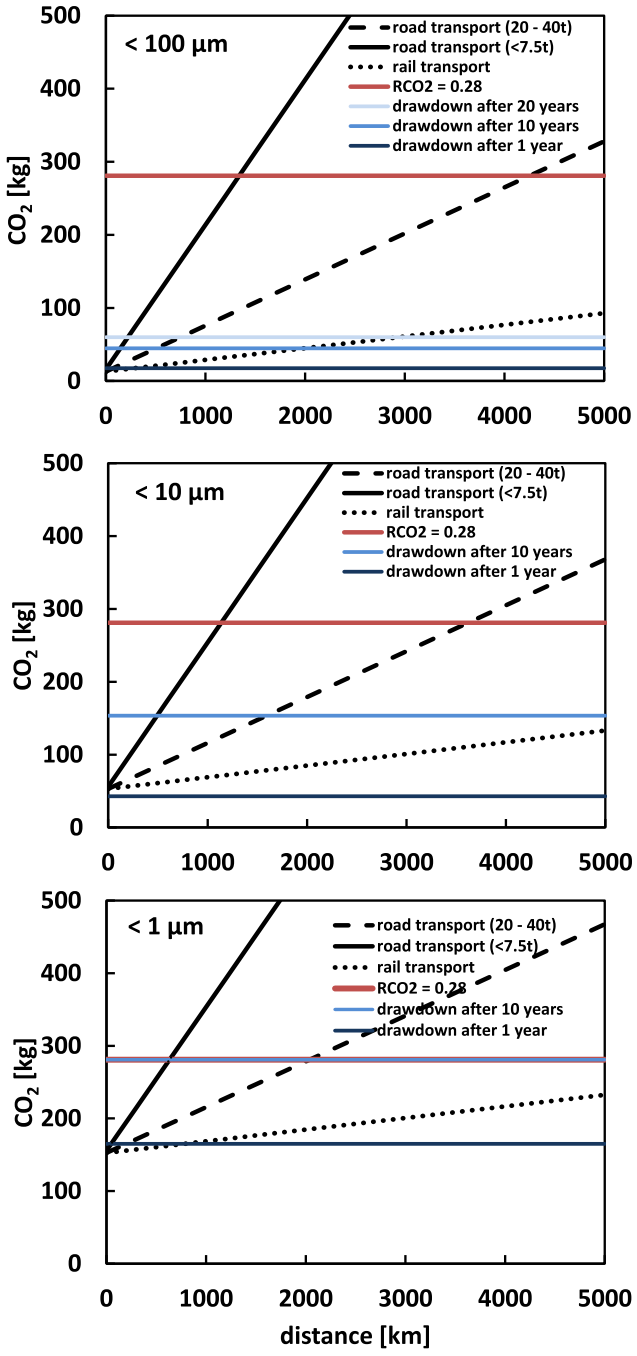

Fig. 7. Relation between grain size dependent weathering and maximum transport distances to offset potential capture. The offsetting distance decreases from 1340 km (<100 µm) to 634 km (<1 µm) for truck transport. However considering the drawdown after 10 years this distance decreases to 161 km for in the <100 µm scenario. For rail transport the offsetting distance decreases from 16,756 km (<100 µm) to 8027 km (<1 µm). Again considering the drawdown after 10 years distance it is only 1993 km (<100 µm).

year 2001, the amount of electricity import was always greater than export. Reducing energy demand is considered one of the key factors in fighting climate change over the next decades and in this context liberating 0.5% of the annual electricity generation for rock comminution will not be an easy task. The use of quarry fines, waste and byproducts from the steel and cement industry as soil fertilizers could partially alleviate this problem as those materials have already been produced in high volumes (Das et al., 2019; Manning et al., 2013; Renforth, 2019; Washbourne et al., 2012). While these potential sources warrant further investigation, large parts of historical wastes may be unavailable for re-extraction (Pullin et al., 2019) and focus should be put on management of future production. In addition, steel slag is already used as an additive to cement, thereby contributing to reducing emissions in the cement industry (Yi et al., 2012). Accordingly, tradeoffs between different forms of reuse have to be considered. We also hypothesize that the application of basalt to agricultural land as natural fertilizer holds a unique advantage compared to other NETs with respect to public acceptance. This advantage might vanish in the case of steel slag and cement waste. Finally, uncertainty in our assessment is related to the energy amount for grinding. The comminution of material to a grainsize in the range of 10 µm could be achieved with lower energy input than assumed in prior publications, given the application of state of the art milling equipment (de Bakker, 2014; Gao et al., 2002). Accordingly, the actual amount of energy used for grinding poses an uncertainty in this study and the need to better constrain this has already been emphasized by (Hartmann et al., 2013).

3.6. The amount of basalt needed

With an assumed density of 3 g cm^{-3}, the 190 Mt basalt that are applied to Austrian land fill a volume of 0.063 km^3 (a cube of approximately 400 m side length). The annual amount of basalt mined in Austria was around 1.5–2 Mt in the years 2015–2018 (Österreichisches Montan-Handbuch, 2019 - *93. Jahrgang*, 2019). The cumulative amount of all mined rocks and minerals amounts to ≈70 Mt a^{-1}. The necessary amount of basalt can most likely not be sustained through mining on Austrian territory, although large volumes of volcanic rock might be found beneath the surface (Heritsch, 1982). In addition, 100 t ha^{-1} is high and it has been shown that considerable CO_2 drawdown can also be achieved with lower application rates (Dietzen et al., 2018; ten Berge et al., 2012), potentially allowing to reduce the amount of basalt. In any case, the mafic lavas of the central European volcanic province in Germany comprise several thousand km^3 (Jung et al., 2005) and the eruptive volume of the Vogelsberg (central Germany) alone is ≈ 600 km^3 (Bogaard et al., 2003). Kereszturi et al. (2011) calculated a volume of volcanic rocks for the Bakony-Balaton Highland Volcanic Field in the Pannonian Carpathian region of ≈2.9 km^3 and large volumes of volcanic rocks are present in the Bohemian Massif, for instance in the Doupov Mountains (123 km^3) (Shrbený, 1995). Conclusively, there is potential for volcanic rock mining in central Europe for several application cycles on agricultural land, not just in Austria. However, mining even if related to sustainable agriculture and climate change mitigation inevitable is in confrontation with other aspects of environmental protection, related to the conservation of nature for ecological, economic and cultural reasons. The enormous touristic potential of some of the regions, by means of cultural heritage, the thermal spa tourism often related to Cenozoic volcanism, agricultural use in general and the high quality wines often related to volcanic terrains in particular put limits on the mining capacity of the regions. In addition, environmental impact assessment of related mining projects can be enduring. Even if a first assessment shows the enormous volumes of volcanic rocks in Central Europe, not every occurrence will provide the desired chemical composition (see Fig. 2), and high quality outcrops are already heavily exploited. Therefore if basalt fertilizer is to play a more prominent role in Austria's (and Europe's) land management practices, strategic planning of the resources use is now warranted on the European level.

4. Conclusion

This study assessed the potential of EW through application of basalt on agricultural land. Two alternative scenarios for basalt with high (R_{CO2_max} = 880 kg CO_2 t^{-1}) and low (R_{CO2_low} = 282 kg CO_2 t^{-1}) CO_2 drawdown potential were evaluated for a single application, a reaction

time of 10 years and three different grain sizes (<100 μm, <10 μm and <1 μm). Using a modified shrinking core model, the CO_2 drawdown in our scenarios after 10 years is lower than in previous estimates. Using a grain size (<100 μm) and R_{CO2_low}, the drawdown is only 45 kg CO_2 per ton of rock. For a transport distance of 300 km the net drawdown of CO_2 ranges with decreasing grain size from 27.3 kg CO_2 t^{-1} (<100 μm) to 125 kg CO_2 t^{-1} (<1 μm) in the R_{CO2_low} scenario, if transport is carried out by railway. The results also indicate, that road transport would turn the application of a <100 μm grain size ineffective or worse, even contribute CO_2 emission. However, transport becomes less important with decreasing grain size. Application of 100 t ha^{-1} with a <10 μm grain size could draw down approximately 2% of Austria's annual greenhouse gas emissions. Grinding of this amount of rock, based on an application cycle of 10 years, would require up to ≈5% of Austria's total annual power generation. Larger grain sizes have been proposed to circumvent this problem, but our results suggest this energy will have to be available if enhanced basalt weathering is to make an impact on the CO_2 budget. However, at the moment, uncertainties related to effective mechanisms of CO_2 consumption during weathering hinder precise quantification. Stoichiometric dissolution of basalt including Al^{3+}, could withdraw higher amounts of CO_2 (R_{CO2_max} = 880 kg CO_2 t^{-1}), in which case the application of larger grain sizes (<100 μm) could be sufficient. Uncertainties regarding the actual field weathering rates of basalt powder in soil further complicate our ability to quantify the CO_2 drawdown related to EW. The precise determination of these rates remains a crucial requirement towards the large scale application of EW. Further studies from laboratory to field scale will be necessary to overcome these deficiencies in order to put the available resources to optimal use within a European strategy. In addition the influence of agricultural practice on greenhouse gas emissions is increasingly put into focus in the context of climate policy, e.g. the EU LULUCF regulation (Romppanen, 2020), and soil amelioration through the application of basalt could become an integral part of soil carbon management. At last, the energy demand related to EW produces an obvious conundrum. EW is in conflict with the need to reduce energy consumption and the necessary phasing out of fossil fuel based energy. As such, EW relies on our transformation into a sustainable society with a low carbon economy and abundant low carbon power supply to contribute to climate change mitigation. It does vice versa not contribute to this transformation.

CRediT authorship contribution statement

Thomas Rinder: Conceptualization, Methodology, Software, Investigation, Writing – original draft, Writing – review & editing, Visualization. **Christoph von Hagke:** Conceptualization, Writing – review & editing.

Declaration of competing interest

The authors declare that they have no known competing financial interests or personal relationships that could have appeared to influence the work reported in this paper.

Acknowledgements

We thank Sylke Hilberg for valuable comments on this manuscript. Diego Bedoya-González and Timo Kessler are thanked for their help with creation of the map. Kayla Iacovino is thanked for providing an excel sheet for plotting TAS diagrams on her website (www.kaylaiacovino.com). We also thank Zhifu Mi and Jing-Li Fan for editorial handling of this manuscripts. 4 anonymous reviewers are thanked for their help in the improvement of this manuscript. This research did not receive any specific grant from funding agencies in the public, commercial, or not-for-profit sectors.

Appendix A. Supplementary data

Supplementary data to this article can be found online at https://doi.org/10.1016/j.jclepro.2021.128178.

References

Adrees, M., Ali, S., Rizwan, M., Zia-ur-Rehman, M., Ibrahim, M., Abbas, F., Farid, M., Qayyum, M.F., Irshad, M.K., 2015. Mechanisms of silicon-mediated alleviation of heavy metal toxicity in plants: a review. Ecotoxicol. Environ. Saf. 119, 186–197. https://doi.org/10.1016/j.ecoenv.2015.05.011.

Ali, S., Ntaflos, T., 2011. Alkali basalts from Burgenland, Austria: petrological constraints on the origin of the westernmost magmatism in the Carpathian-Pannonian Region. Lithos 121, 176–188. https://doi.org/10.1016/j.lithos.2010.11.001.

Ali, S., Ntaflos, T., Upton, B.G.J., 2013. Petrogenesis and mantle source characteristics of Quaternary alkaline mafic lavas in the western Carpathian-Pannonian Region, Styria, Austria. Chem. Geol. 337–338, 99–113. https://doi.org/10.1016/j.chemgeo.2012.12.001.

Alibert, C., Michard, A., Albarède, F., 1983. The transition from alkali basalts to kimberlites: isotope and trace element evidence from melilitites. Contrib. Mineral. Petrol. 82, 176–186.

Amann, T., Hartmann, J., 2019. Ideas and perspectives: synergies from co-deployment of negative emission technologies. Biogeosciences 16, 2949–2960. https://doi.org/10.5194/bg-16-2949-2019.

Amann, T., Hartmann, J., Struyf, E., de Oliveira Garcia, W., Fischer, E.K., Janssens, I.A., Meire, P.M., Schoelynck, J., 2020. Enhanced Weathering and related element fluxes-A cropland mesocosm approach. Biogeosciences 17, 103–119. https://doi.org/10.5194/bg-17-103-2020.

Amiotte Suchet, P., Probst, J.-L., Ludwig, W., 2003. Worldwide distribution of continental rock lithology: implications for the atmospheric/soil CO_2 uptake by continental weathering and alkalinity river transport to the oceans. Global Biogeochem. Cycles 17. https://doi.org/10.1029/2002GB001891.

Anderson, K., Broderick, J.F., Stoddard, I., 2020. A factor of two: how the mitigation plans of 'climate progressive' nations fall far short of Paris-compliant pathways. Clim. Pol. 1–15. https://doi.org/10.1080/14693062.2020.1728209.

Anderson, K., Peters, G., 2016. The Trouble with Negative Emissions. INSIGHTS | Perspect, vol. 182. https://doi.org/10.1007/s10484-016-1770-6.

Asch, K., 2005. GME 5000: 1 : 5 Million International Geological Map of Europe and Adjacent Areas. BGR.

Assima, G.P., Larachi, F., Beaudoin, G., Molson, J., 2012. CO_2 sequestration in chrysotile mining residues-implication of watering and passivation under environmental conditions. Ind. Eng. Chem. Res. 51, 8726–8734. https://doi.org/10.1021/ie202693q.

Assima, G.P., Larachi, F., Molson, J., Beaudoin, G., 2014. Comparative study of five Québec ultramafic mining residues for use in direct ambient carbon dioxide mineral sequestration. Chem. Eng. J. 245, 56–64. https://doi.org/10.1016/j.cej.2014.02.010.

Aviso, K.B., Lee, J.-Y., Ubando, A.T., Tan, R.R., 2021. Fuzzy optimization model for enhanced weathering networks using industrial waste. Clean Technol. Environ. Policy. https://doi.org/10.1007/s10098-021-02053-8.

Babechuk, M.G., Widdowson, M., Kamber, B.S., 2014. Quantifying chemical weathering intensity and trace element release from two contrasting basalt profiles, Deccan Traps, India. Chem. Geol. 363, 56–75.

Bach, L.T., Gill, S.J., Rickaby, R.E.M., Gore, S., Renforth, P., 2019. CO_2 removal with enhanced weathering and ocean alkalinity enhancement: potential risks and Co-benefits for marine pelagic ecosystems. Front. Clim. 1, 7. https://doi.org/10.3389/fclim.2019.00007.

Beccaluva, L., Di Girolamo, P., Serri, G., 1991. Petrogenesis and tectonic setting of the roman volcanic province, Italy. Lithos 26, 191–221. https://doi.org/10.1016/0024-4937(91)90029-K.

Beerling, D.J., 2017. Enhanced rock weathering: biological climate change mitigation with co-benefits for food security? Biol. Lett. https://doi.org/10.1098/rsbl.2017.0149.

Beerling, D.J., Kantzas, E.P., Lomas, M.R., Wade, P., Eufrasio, R.M., Renforth, P., Sarkar, B., Andrews, M.G., James, R.H., Pearce, C.R., Mercure, J.F., Pollitt, H., Holden, P.B., Edwards, N.R., Khanna, M., Koh, L., Quegan, S., Pidgeon, N.F., Janssens, I.A., Hansen, J., Banwart, S.A., 2020. Potential for large-scale CO_2 removal via enhanced rock weathering with croplands. Nature 583, 242–248. https://doi.org/10.1038/s41586-020-2448-9.

Beerling, D.J., Leake, J.R., Long, S.P., Scholes, J.D., Ton, J., Nelson, P.N., Bird, M., Kantzas, E., Taylor, L.L., Sarkar, B., Kelland, M., DeLucia, E., Kantola, I., Müller, C., Rau, G., Hansen, J., 2018. Farming with crops and rocks to address global climate, food and soil security/631/449/706/1143/704/47/704/106 perspective. Native Plants 4, 138–147. https://doi.org/10.1038/s41477-018-0108-y.

Berner, R.A., Lasaga, A.C., Garrels, R.M., 1983. The carbonate-silicate geochemical cycle and its effect on atmospheric carbon dioxide over the past 100 million years. Am. J. Sci. 283, 641–683.

Bickmore, B.R., Nagy, K.L., Gray, A.K., Brinkerhoff, A.R., 2006. The effect of $Al(OH)_4^-$ on the dissolution rate of quartz. Geochem. Cosmochim. Acta 70, 290–305. https://doi.org/10.1016/J.GCA.2005.09.017.

Bogaard, P.J.F., Wo, G., Rnery, È., 2003. Petrogenesis of basanitic to tholeiitic volcanic rocks from the miocene Vogelsberg, Central Germany. Journal of Petrology. Oxford Academic.

Brantley, S.L., Mellott, N.P., 2000. Surface area and porosity of primary silicate minerals. Am. Mineral. 85, 1767–1783. https://doi.org/10.2138/am-2000-11-1220.
Briot, D., Cantagrel, J.M., Dupuy, C., Harmon, R.S., 1991. Geochemical evolution in crustal magma reservoirs: trace-element and Sr-Nd-O isotopic variations in two continental intraplate series at Monts Dore, Massif Central, France. Chem. Geol. 89, 281–303.
Brunauer, S., Emmett, P.H., Teller, E., 1938. Adsorption of gases in multimolecular layers. J. Am. Chem. Soc. 60, 309–319. https://doi.org/10.1021/ja01269a023.
Chauvel, C., Jahn, B.-M., 1984. Nd-Sr isotope and REE geochemistry of alkali basalts from the Massif Central, France. Geochem. Cosmochim. Acta 48, 93–110.
Chernyshev, I.V., Konečný, V., Lexa, J., Kovalenker, V.A., Jeleň, S., Lebedev, V.A., Goltsman, Y.V., 2013. K-Ar and Rb-Sr geochronology and evolution of the Štiavnica stratovolcano (Central Slovakia). Geol. Carpathica 64, 327–360.
Cocker, K.M., Evans, D.E., Hodson, M.J., 1998. The amelioration of aluminium toxicity by silicon in higher plants: solution chemistry or an in planta mechanism? Physiol. Plant. 104, 608–614. https://doi.org/10.1034/j.1399-3054.1998.1040413.x.
Cortesogno, L., Cassinis, G., Dallagiovanna, G., Gaggero, L., Oggiano, G., Ronchi, A., Seno, S., Vanossi, M., 1998. The variscan post-collisional volcanism in late carboniferous–permian sequences of Ligurian alps, southern alps and sardinia (Italy): a synthesis. Lithos 45, 305–328. https://doi.org/10.1016/S0024-4937(98)00037-1.
Das, A., Krishnaswami, S., Sarin, M.M., Pande, K., 2005. Chemical weathering in the krishna basin and western ghats of the Deccan Traps, India: rates of basalt weathering and their controls. Geochem. Cosmochim. Acta 69, 2067–2084. https://doi.org/10.1016/j.gca.2004.10.014.
Das, S., Kim, G.W., Hwang, H.Y., Verma, P.P., Kim, P.J., 2019. Cropping with slag to address soil, environment, and food security. Front. Microbiol. https://doi.org/10.3389/fmicb.2019.01320.
Dautria, J.-M., Liotard, J.-M., Briot, D., 2004. Particularités de la contamination crustale des phonolites: exemple du Velay oriental (Massif central). Compt. Rendus Geosci. 336, 971–981.
Daval, D., Calvaruso, C., Guyot, F., Turpault, M.P., 2018. Time-dependent feldspar dissolution rates resulting from surface passivation: experimental evidence and geochemical implications. Earth Planet Sci. Lett. 498, 226–236. https://doi.org/10.1016/j.epsl.2018.06.035.
Daval, D., Hellmann, R., Saldi, G.D., Wirth, R., Knauss, K.G., 2013. Linking nm-scale measurements of the anisotropy of silicate surface reactivity to macroscopic dissolution rate laws: new insights based on diopside. Geochem. Cosmochim. Acta 107, 121–134. https://doi.org/10.1016/j.gca.2012.12.045.
de Bakker, J., 2014. Energy use of fine grinding in mineral processing. Metall. Mater. Trans. 1, 8–19. https://doi.org/10.1007/s40553-013-0001-6.
Dessert, C., Dupré, B., François, L.M., Schott, J., Gaillardet, J., Chakrapani, G., Bajpai, S., 2001. Erosion of Deccan Traps determined by river geochemistry: impact on the global climate and the $^{87}Sr/^{86}Sr$ ratio of seawater. Earth Planet Sci. Lett. 188, 459–474.
Dessert, C., Dupré, B., Gaillardet, J., François, L.M., Allègre, C.J., 2003. Basalt weathering laws and the impact of basalt weathering on the global carbon cycle. Chem. Geol. 202, 257–273. https://doi.org/10.1016/j.chemgeo.2002.10.001.
Dietzen, C., Harrison, R., Michelsen-Correa, S., 2018. Effectiveness of enhanced mineral weathering as a carbon sequestration tool and alternative to agricultural lime: an incubation experiment. Int. J. Greenh. Gas Control 74, 251–258. https://doi.org/10.1016/j.ijggc.2018.05.007.
Downes, H., Seghedi, I., Szakacs, A., Dobosi, G., James, D.E., Vaselli, O., Rigby, I.J., Ingram, G.A., Rex, D., Pecskay, Z., 1995. Petrology and geochemistry of late Tertiary/Quaternary mafic alkaline volcanism in Romania. Lithos 35, 65–81. https://doi.org/10.1016/0024-4937(95)91152-Y.
Echevarria, G., 2018. Genesis and Behaviour of Ultramafic Soils and Consequences for Nickel Biogeochemistry. Springer, Cham, pp. 135–156. https://doi.org/10.1007/978-3-319-61899-9_8.
Elliot Smith, M., Carroll, A.R., Mueller, E.R., 2008. Elevated weathering rates in the rocky Mountains during the early eocene climatic optimum. Nat. Geosci. 1, 370–374. https://doi.org/10.1038/ngeo205.
Emissions Gap Report 2019, 2019. Nairobi.
Fuss, S., Canadell, J.G., Peters, G.P., Tavoni, M., Andrew, R.M., Ciais, P., Jackson, R.B., Jones, C.D., Kraxner, F., Nakicenovic, N., Le Quéré, C., Raupach, M.R., Sharifi, A., Smith, P., Yamagata, Y., 2014. COMMENTARY: betting on negative emissions. Nat. Clim. Chang.
Fuss, S., William, F.L., Max, W.C., Jérôme, H., Felix, C., Thorben, A., Tim, B., Wagner de Oliveira, G., Jens, H., Tarun, K., Gunnar, L., Gregory, F.N., Joeri, R., Pete, S., José Luis Vicente, V., Jennifer, W., Maria del Mar Zamora, D., Jan, C.M., 2018. Negative emissions—Part 2: costs, potentials and side effects. Environ. Res. Lett. 13, 63002.
Gaillardet, J., Dupré, B., Louvat, P., Allègre, C.J., 1999. Global silicate weathering and CO_2 consumption rates deduced from the chemistry of large rivers. Chem. Geol. 159, 3–30. https://doi.org/10.1016/S0009-2541(99)00031-5.
Galeczka, I., Wolff-Boenisch, D., Oelkers, E.H., Gislason, S.R., 2014. An experimental study of basaltic glass–H_2O–CO_2 interaction at 22 and 50°C: implications for subsurface storage of CO_2. Geochem. Cosmochim. Acta 126, 123–145. https://doi.org/10.1016/j.gca.2013.10.044.
Gao, M., Young, M., Allum, P., 2002. IsaMill fine grinding technology and its industrial applications at Mount Isa Mines. In: 34th Annual Meeting of the Canadian Mineral Processors.
Gautier, J.-M., Oelkers, E.H., Schott, J., 1994. Experimental study of K-feldspar dissolution rates as a function of chemical affinity at 150°C and pH 9. Geochem. Cosmochim. Acta 58, 4549–4560. https://doi.org/10.1016/0016-7037(94)90190-2.
Gerdemann, S.J., O'Connor, W.K., Dahlin, D.C., Penner, L.R., Rush, H., 2007. Ex situ aqueous mineral carbonation. Environ. Sci. Technol. 41, 2587–2593. https://doi.org/10.1021/es0619253.
Gerrits, R., Wirth, R., Schreiber, A., Feldmann, I., Knabe, N., Schott, J., Benning, L.G., Gorbushina, A.A., 2020. High-resolution imaging of fungal biofilm-induced olivine weathering. Chem. Geol. 119902. https://doi.org/10.1016/j.chemgeo.2020.119902.
Gillman, G.P., Burkett, D.C., Coventry, R.J., 2002. Amending highly weathered soils with finely ground basalt rock. In: Applied Geochemistry. Pergamon, pp. 987–1001. https://doi.org/10.1016/S0883-2927(02)00078-1.
Gislason, S.R., Oelkers, E.H., 2003. Mechanism, rates, and consequences of basaltic glass dissolution: II. An experimental study of the dissolution rates of basaltic glass as a function of pH and temperature. Geochem. Cosmochim. Acta 67, 3817–3832. https://doi.org/10.1016/s0016-7037(03)00176-5.
Gislason, S.R., Oelkers, E.H., Eiriksdottir, E.S., Kardjilov, M.I., Gisladottir, G., Sigfusson, B., Snorrason, A., Elefsen, S., Hardardottir, J., Torssander, P., Oskarsson, N., 2009. Direct evidence of the feedback between climate and weathering. Earth Planet Sci. Lett. 277, 213–222. https://doi.org/10.1016/j.epsl.2008.10.018.
Gras, A., Beaudoin, G., Molson, J., Plante, B., 2020. Atmospheric carbon sequestration in ultramafic mining residues and impacts on leachate water chemistry at the Dumont Nickel Project, Quebec, Canada. Chem. Geol. 119661. https://doi.org/10.1016/j.chemgeo.2020.119661.
Gudbrandsson, S., Wolff-Boenisch, D., Gislason, S.R., Oelkers, E.H., 2014. Experimental determination of plagioclase dissolution rates as a function of its composition and pH at 22°C. Geochem. Cosmochim. Acta 139, 154–172. https://doi.org/10.1016/j.gca.2014.04.028.
Gudbrandsson, S., Wolff-Boenisch, D., Gislason, S.R., Oelkers, E.H., 2011. An experimental study of crystalline basalt dissolution from 2≤ pH≤ 11 and temperatures from 5 to 75° C. Geochem. Cosmochim. Acta 75, 5496–5509. https://doi.org/10.1016/j.gca.2011.06.035.
Guntzer, F., Keller, C., Meunier, J.D., 2012. Benefits of plant silicon for crops: a review. Agron. Sustain. Dev. https://doi.org/10.1007/s13593-011-0039-8.
Gwenzi, W., 2020. Occurrence, behaviour, and human exposure pathways and health risks of toxic geogenic contaminants in serpentinitic ultramafic geological environments (SUGEs): a medical geology perspective. Sci. Total Environ. 700, 134622. https://doi.org/10.1016/j.scitotenv.2019.134622.
Haase, K.M., Beier, C., Regelous, M., Rapprich, V., Renno, A., 2017. Spatial variability of source composition and petrogenesis in rift and rift flank alkaline lavas from the Eger Rift, Central Europe. Chem. Geol. 455, 304–314. https://doi.org/10.1016/j.chemgeo.2016.11.003.
Haase, K.M., Goldschmidt, B., Garbe-Schönberg, C.-D., 2004. Petrogenesis of Tertiary continental intra-plate lavas from the Westerwald region, Germany. J. Petrol. 45, 883–905.
Hamilton, J.L., Wilson, S.A., Morgan, B., Turvey, C.C., Paterson, D.J., Jowitt, S.M., McCutcheon, J., Southam, G., 2018. Fate of transition metals during passive carbonation of ultramafic mine tailings via air capture with potential for metal resource recovery. Int. J. Greenh. Gas Control 71, 155–167. https://doi.org/10.1016/j.ijggc.2018.02.008.
Hangx, S.J.T., Spiers, C.J., 2009. Coastal spreading of olivine to control atmospheric CO2 concentrations: a critical analysis of viability. Int. J. Greenh. Gas Control 3, 757–767. https://doi.org/10.1016/j.ijggc.2009.07.001.
Haque, F., Santos, R.M., Chiang, Y.W., 2020a. CO2 sequestration by wollastonite-amended agricultural soils – an Ontario field study. Int. J. Greenh. Gas Control 97, 103017. https://doi.org/10.1016/j.ijggc.2020.103017.
Haque, F., Santos, R.M., Chiang, Y.W., 2020b. Optimizing inorganic carbon sequestration and crop yield with wollastonite soil amendment in a microplot study. Front. Plant Sci. 11, 1012. https://doi.org/10.3389/fpls.2020.01012.
Haque, F., Santos, R.M., Dutta, A., Thimmanagari, M., Chiang, Y.W., 2019. Co-benefits of wollastonite weathering in agriculture: CO_2 sequestration and promoted plant growth. ACS Omega 4, 1425–1433.
Harangi, S., Downes, H., Thirlwall, M., Gméling, K., 2007. Geochemistry, petrogenesis and geodynamic relationships of miocene calc-alkaline volcanic rocks in the western carpathian arc, eastern central Europe. J. Petrol. 48, 2261–2287. https://doi.org/10.1093/petrology/egm059.
Harangi, S., Jankovics, M.É., Sági, T., Kiss, B., Lukács, R., Soós, I., 2015. Origin and geodynamic relationships of the Late Miocene to Quaternary alkaline basalt volcanism in the Pannonian basin, eastern–central Europe. Int. J. Earth Sci. 104, 2007–2032.
Harrison, A.L., Dipple, G.M., Power, I.M., Mayer, K.U., 2015. Influence of surface passivation and water content on mineral reactions in unsaturated porous media: implications for brucite carbonation and CO_2 sequestration. Geochem. Cosmochim. Acta 148, 477–495. https://doi.org/10.1016/j.gca.2014.10.020.
Harrison, A.L., Dipple, G.M., Song, W., Power, I.M., Mayer, K.U., Beinlich, A., Sinton, D., 2017. Changes in mineral reactivity driven by pore fluid mobility in partially wetted porous media. Chem. Geol. 463, 1–11. https://doi.org/10.1016/j.chemgeo.2017.05.003.
Harrison, A.L., Power, I.M., Dipple, G.M., 2013. Accelerated carbonation of brucite in mine tailings for carbon sequestration. Environ. Sci. Technol. 47, 126–134. https://doi.org/10.1021/es3012854.
Hartmann, J., Moosdorf, N., 2012. The new global lithological map database GLiM: a representation of rock properties at the Earth surface. G-cubed 13.
Hartmann, J., West, A.J., Renforth, P., Köhler, P., De La Rocha, C.L., Wolf-Gladrow, D.A., Dürr, H.H., Scheffran, J., 2013. Enhanced chemical weathering as a geoengineering strategy to reduce atmospheric carbon dioxide, supply nutrients, and mitigate ocean acidification. Rev. Geophys. 51, 113–149. https://doi.org/10.1002/rog.20004.

Hegner, E., Walter, H.J., Satir, M., 1995. Pb-Sr-Nd isotopic compositions and trace element geochemistry of megacrysts and melilitites from the Tertiary Urach volcanic field: source composition of small volume melts under SW Germany. Contrib. Mineral. Petrol. 122, 322–335.
Hensel, J., 1894. Bread from Stones [from old catalog]. A. J. Tafel, Philadelphia, Pa. https://doi.org/10.5962/bhl.title.42970. Bread from stones.
Heritsch, H., 1982. Die Latite aus der Tiefbohrung in Bad Gleichenberg, Steiermark. Mitt. naturwiss. Ver. Steiermark 112, 27–47.
Hickel, J., Kallis, G., 2020. Is green growth possible? New polit. Econ. Times 25, 469–486. https://doi.org/10.1080/13563467.2019.1598964.
Hilaire, J., Minx, J.C., Callaghan, M.W., Edmonds, J., Luderer, G., Nemet, G.F., Rogelj, J., del Mar Zamora, M., 2019. Negative emissions and international climate goals—learning from and about mitigation scenarios. Climatic Change 157, 189–219. https://doi.org/10.1007/s10584-019-02516-4.
Hotchkiss, E.R., Hall Jr., R.O., Sponseller, R.A., Butman, D., Klaminder, J., Laudon, H., Rosvall, M., Karlsson, J., 2015. Sources of and processes controlling CO_2 emissions change with the size of streams and rivers. Nat. Geosci. 8, 696–699. https://doi.org/10.1038/ngeo2507.
Iler, R., 1973. Effect of adsorbed alumina on the solubility of amorphous silica in water. J. Colloid Interface Sci. 43, 399–408. https://doi.org/10.1016/0021-9797(73)90386-X.
Jung, C., Jung, S., Hoffer, E., Berndt, J., 2006. Petrogenesis of Tertiary mafic alkaline magmas in the Hocheifel, Germany. J. Petrol. 47, 1637–1671. https://doi.org/10.1093/petrology/egl023.
Jung, S., Masberg, P., 1998. Major- and trace-element systematics and isotope geochemistry of Cenozoic mafic volcanic rocks from the Vogelsberg (central Germany): constraints on the origin of continental alkaline and tholeiitic basalts and their mantle sources. J. Volcanol. Geoth. Res. 86, 151–177. https://doi.org/10.1016/S0377-0273(98)00087-0.
Jung, S., Pfänder, J.A., Brügmann, G., Stracke, A., 2005. Sources of primitive alkaline volcanic rocks from the Central European Volcanic Province (Rhön, Germany) inferred from Hf, Os and Pb isotopes. Contrib. Mineral. Petrol. 150, 546–559.
Kantola, I.B., Masters, M.D., Beerling, D.J., Long, S.P., DeLucia, E.H., 2017. Potential of global croplands and bioenergy crops for climate change mitigation through deployment for enhanced weathering. Biol. Lett. 13, 20160714. https://doi.org/10.1098/rsbl.2016.0714.
Kelemen, P.B., McQueen, N., Wilcox, J., Renforth, P., Dipple, G., Vankeuren, A.P., 2020. Engineered carbon mineralization in ultramafic rocks for CO_2 removal from air: review and new insights. Chem. Geol. 550, 119628. https://doi.org/10.1016/j.chemgeo.2020.119628.
Kelland, M.E., Wade, P.W., Lewis, A.L., Taylor, L.L., Sarkar, B., Andrews, M.G., Lomas, M.R., Cotton, T.E.A., Kemp, S.J., James, R.H., Pearce, C.R., Hartley, S.E., Hodson, M.E., Leake, J.R., Banwart, S.A., Beerling, D.J., 2020. Increased yield and CO_2 sequestration potential with the C4 cereal Sorghum bicolor cultivated in basaltic rock dust-amended agricultural soil. Global Change Biol. 26, 3658–3676. https://doi.org/10.1111/gcb.15089.
Kereszturi, G., Németh, K., Csillag, G., Balogh, K., Kovács, J., 2011. The role of external environmental factors in changing eruption styles of monogenetic volcanoes in a Mio/Pleistocene continental volcanic field in western Hungary. J. Volcanol. Geoth. Res. 201, 227–240. https://doi.org/10.1016/j.jvolgeores.2010.08.018.
Kierczak, J., Pedziwiatr, A., Waroszewski, J., Modelska, M., 2016. Mobility of Ni, Cr and Co in serpentine soils derived on various ultrabasic bedrocks under temperate climate. Geoderma 268, 78–91. https://doi.org/10.1016/j.geoderma.2016.01.025.
Köhler, P., Hartmann, J., Wolf-Gladrow, D.A., 2010. Geoengineering potential of artificially enhanced silicate weathering of olivine. Proc. Natl. Acad. Sci. U. S. A. 107, 20228–20233. https://doi.org/10.1073/pnas.1000545107.
Kump, L.R., Arthur, M.A., Patzkowsky, M.E., Gibbs, M.T., Pinkus, D.S., Sheehan, P.M., 1999. A weathering hypothesis for glaciation at high atmospheric pCO_2 during the Late Ordovician. Palaeogeogr. Palaeoclimatol. Palaeoecol. 152, 173–187. https://doi.org/10.1016/S0031-0182(99)00046-2.
Lackner, K.S., Wendt, C.H., Butt, D.P., Joyce, E.L., Sharp, D.H., 1995. Carbon dioxide disposal in carbonate minerals. Energy 20, 1153–1170. https://doi.org/10.1016/0360-5442(95)00071-N.
Lechat, K., Lemieux, J.-M., Molson, J., Beaudoin, G., Hébert, R., 2016. Field evidence of CO_2 sequestration by mineral carbonation in ultramafic milling wastes, Thetford Mines, Canada. Int. J. Greenh. Gas Control 47, 110–121. https://doi.org/10.1016/j.ijggc.2016.01.036.
Lefebvre, D., Goglio, P., Williams, A., Manning, D.A.C., de Azevedo, A.C., Bergmann, M., Meersmans, J., Smith, P., 2019. Assessing the potential of soil carbonation and enhanced weathering through Life Cycle Assessment: a case study for Sao Paulo State, Brazil. J. Clean. Prod. 233, 468–481. https://doi.org/10.1016/j.jclepro.2019.06.099.
Li, Gaojun, Hartmann, J., Derry, L.A., West, A.J., You, C.-F., Long, X., Zhan, T., Li, L., Li, Gen, Qiu, W., Li, T., Liu, L., Chen, Y., Ji, J., Zhao, L., Chen, J., 2016. Temperature dependence of basalt weathering. Earth Planet Sci. Lett. 443, 59–69. https://doi.org/10.1016/j.epsl.2016.03.015.
Liang, Y.C., Ma, T.S., Li, F.J., Feng, Y.J., 1994. Silicon availability and response of rice and wheat to silicon in calcareous soils. Commun. Soil Sci. Plant Anal. 25, 2285–2297.
Louvat, P., Allègre, C.J., 1997. Present denudation rates on the island of Reunion determined by river geochemistry: basalt weathering and mass budget between chemical and mechanical erosions. Geochem. Cosmochim. Acta 61, 3645–3669.
Lowe, D.R., Tice, M.M., 2004. Geologic evidence for Archean atmospheric and climatic evolution: fluctuating levels of CO_2, CH_4, and O_2 with an overriding tectonic control. Geology 32, 493–496. https://doi.org/10.1130/G20342.1.
Lukács, R., Harangi, S., Guillong, M., Bachmann, O., Fodor, L., Buret, Y., Dunkl, I., Sliwinski, J., von Quadt, A., Peytcheva, I., Zimmerer, M., 2018. Early to Mid-Miocene syn-extensional massive silicic volcanism in the Pannonian Basin (East-Central Europe): eruption chronology, correlation potential and geodynamic implications. Earth Sci. Rev. 179, 1–19. https://doi.org/10.1016/j.earscirev.2018.02.005.
Lustrino, M., Wilson, M., 2007. The circum-Mediterranean anorogenic Cenozoic igneous province. Earth Sci. Rev. 81, 1–65. https://doi.org/10.1016/j.earscirev.2006.09.002.
Macera, P., Gasperini, D., Piromallo, C., Blichert-Toft, J., Bosch, D., Del Moro, A., Martin, S., 2003. Geodynamic implications of deep mantle upwelling in the source of Tertiary volcanics from the Veneto region (South-Eastern Alps). J. Geodyn. 36, 563–590.
Maher, K., 2010. The dependence of chemical weathering rates on fluid residence time. Earth Planet Sci. Lett. 294, 101–110. https://doi.org/10.1016/j.epsl.2010.03.010.
Maher, K., Steefel, C.I., White, A.F., Stonestrom, D.A., 2009. The role of reaction affinity and secondary minerals in regulating chemical weathering rates at the Santa Cruz Soil Chronosequence, California. Geochem. Cosmochim. Acta 73, 2804–2831. https://doi.org/10.1016/j.gca.2009.01.030.
Manning, D.A.C., Renforth, P., Lopez-Capel, E., Robertson, S., Ghazireh, N., 2013. Carbonate precipitation in artificial soils produced from basaltic quarry fines and composts: an opportunity for passive carbon sequestration. Int. J. Greenh. Gas Control 17, 309–317.
Marx, A., Dusek, J., Jankovec, J., Sanda, M., Vogel, T., van Geldern, R., Hartmann, J., Barth, J.A.C., 2017. A review of CO_2 and associated carbon dynamics in headwater streams: a global perspective. Rev. Geophys. 55, 560–585. https://doi.org/10.1002/2016RG000547.
Mertes, H., Schmincke, H.-U., 1985. Mafic potassic lavas of the Quaternary West Eifel volcanic field. Contrib. Mineral. Petrol. 89, 330–345.
Milani, L., Beccaluva, L., Coltorti, M., 1999. Petrogenesis and evolution of the euganean magmatic complex, Veneto region, north-east Italy. Eur. J. Mineral 11, 379–399.
Montserrat, F., Renforth, P., Hartmann, J., Leermakers, M., Knops, P., Meysman, F.J.R., 2017. Olivine dissolution in seawater: implications for CO_2 sequestration through enhanced weathering in coastal environments. Environ. Sci. Technol. 51, 3960–3972.
Moosdorf, N., Renforth, P., Hartmann, J., 2014. Carbon dioxide efficiency of terrestrial enhanced weathering. Environ. Sci. Technol. 48, 4809–4816. https://doi.org/10.1021/es4052022.
Moulton, K.L., West, J., Berner, R.A., 2000. Solute flux and mineral mass balance approaches to the quantification of plant effects on silicate weathering. Am. J. Sci. 300, 539–570. https://doi.org/10.2475/ajs.300.7.539.
Navarre-Sitchler, A., Brantley, S., 2007. Basalt weathering across scales. Earth Planet Sci. Lett. 261, 321–334.
Navarre-Sitchler, A., Steefel, C.I., Sak, P.B., Brantley, S.L., 2011. A reactive-transport model for weathering rind formation on basalt. Geochem. Cosmochim. Acta 75, 7644–7667. https://doi.org/10.1016/j.gca.2011.09.033.
Negative Emissions Technologies and Reliable Sequestration: A Research Agenda, 2019. Negative Emissions Technologies and Reliable Sequestration. National Academies Press. https://doi.org/10.17226/25259.
Oelkers, E.H., Declercq, J., Saldi, G.D., Gislason, S.R., Schott, J., 2018. Olivine dissolution rates: a critical review. Chem. Geol. 500, 1–19. https://doi.org/10.1016/j.chemgeo.2018.10.008.
Oelkers, E.H., Gislason, S.R., 2001. The mechanism, rates and consequences of basaltic glass dissolution: I. An experimental study of the dissolution rates of basaltic glass as a function of aqueous Al, Si and oxalic acid concentration at 25°C and pH = 3 and 11. Geochem. Cosmochim. Acta 65, 3671–3681. https://doi.org/10.1016/S0016-7037(01)00664-0.
Oelkers, E.H., Schott, J., 2001. An experimental study of enstatite dissolution rates as a function of pH, temperature, and aqueous Mg and Si concentration, and the mechanism of pyroxene/pyroxenoid dissolution. Geochem. Cosmochim. Acta 65, 1219–1231.
Oskierski, H.C., Dlugogorski, B.Z., Oliver, T.K., Jacobsen, G., 2016. Chemical and isotopic signatures of waters associated with the carbonation of ultramafic mine tailings, Woodsreef Asbestos Mine, Australia. Chem. Geol. 436, 11–23.
Österreichisches, 2019. Montan-Handbuch 2019. Jahrgang, p. 93.
Peccerillo, A., 2005. Plio-quaternary Volcanism in Italy. Springer.
Perez-Fodich, A., Derry, L.A., 2019. Organic acids and high soil CO_2 drive intense chemical weathering of Hawaiian basalts: insights from reactive transport models. Geochem. Cosmochim. Acta 249, 173–198. https://doi.org/10.1016/j.gca.2019.01.027.
Perez, A., Rossano, S., Trcera, N., Verney-Carron, A., Huguenot, D., van Hullebusch, E.D., Catillon, G., Razafitianamaharavo, A., Guyot, F., 2015. Impact of iron chelators on short-term dissolution of basaltic glass. Geochem. Cosmochim. Acta 162, 83–98. https://doi.org/10.1016/j.gca.2015.04.025.
Plata, L.G., Ramos, C.G., Silva Oliveira, M.L., Silva Oliveira, L.F., 2021. Release kinetics of multi-nutrients from volcanic rock mining by-products: evidences for their use as a soil remineralizer. J. Clean. Prod. 279, 123668. https://doi.org/10.1016/j.jclepro.2020.123668.
Pokrovsky, O.S., Schott, J., 2000. Kinetics and mechanism of forsterite dissolution at 25 °C and pH from 1 to 12. Geochem. Cosmochim. Acta 64, 3313–3325.
Polsenaere, P., Savoye, N., Etcheber, H., Canton, M., Poirier, D., Bouillon, S., Abril, G., 2013. Export and degassing of terrestrial carbon through watercourses draining a temperate podzolized catchment. Aquat. Sci. 75, 299–319. https://doi.org/10.1007/s00027-012-0275-2.
Power, I.M., Dipple, G.M., Bradshaw, P.M.D., Harrison, A.L., 2020. Prospects for CO_2 mineralization and enhanced weathering of ultramafic mine tailings from the

Baptiste nickel deposit in British Columbia, Canada. Int. J. Greenh. Gas Control 94, 102895.
Prelević, D., Foley, S.F., Romer, R.L., Cvetković, V., Downes, H., 2005. Tertiary ultrapotassic volcanism in Serbia: constraints on petrogenesis and mantle source characteristics. J. Petrol. 46, 1443–1487. https://doi.org/10.1093/petrology/egi022.
Pronost, J., Beaudoin, G., Tremblay, J., Larachi, F., Duchesne, J., Hébert, R., Constantin, M., 2011. Carbon sequestration kinetic and storage capacity of ultramafic mining waste. Environ. Sci. Technol. 45, 9413–9420.
Pullin, H., Bray, A.W., Burke, I.T., Muir, D.D., Sapsford, D.J., Mayes, W.M., Renforth, P., 2019. Atmospheric carbon capture performance of Legacy iron and steel waste. Environ. Sci. Technol. 53, 9502–9511. https://doi.org/10.1021/acs.est.9b01265.
Raymo, M.E., Ruddiman, W.F., 1992. Tectonic forcing of late Cenozoic climate. Nature 359, 117–122. https://doi.org/10.1038/359117a0.
Renforth, P., 2019. The negative emission potential of alkaline materials. Nat. Commun. 10, 1–8. https://doi.org/10.1038/s41467-019-09475-5.
Renforth, P., 2012. The potential of enhanced weathering in the UK. Int. J. Greenh. Gas Control 10, 229–243. https://doi.org/10.1016/j.ijggc.2012.06.011.
Renforth, P., Henderson, G., 2017. Assessing ocean alkalinity for carbon sequestration. Rev. Geophys. 55, 636–674. https://doi.org/10.1002/2016RG000533.
Renforth, P., Pogge von Strandmann, P.A.E., Henderson, G.M., 2015. The dissolution of olivine added to soil: implications for enhanced weathering. Appl. Geochem. 61, 109–118. https://doi.org/10.1016/j.apgeochem.2015.05.016.
Rigopoulos, I., Harrison, A.L., Delimitis, A., Ioannou, I., Efstathiou, A.M., Kyratsi, T., Oelkers, E.H., 2018a. Carbon sequestration via enhanced weathering of peridotites and basalts in seawater. Appl. Geochem. 91, 197–207. https://doi.org/10.1016/j.apgeochem.2017.11.001.
Rigopoulos, I., Török, Á., Kyratsi, T., Delimitis, A., Ioannou, I., 2018b. Sustainable exploitation of mafic rock quarry waste for carbon sequestration following ball milling. Resour. Pol. 59, 24–32. https://doi.org/10.1016/j.resourpol.2018.08.002.
Riley, T.R., Bailey, D.K., Harmer, R.E., Liebsch, H., Lloyd, F.E., Palmer, M.R., 1999. Isotopic and geochemical investigation of a carbonatite-syenite-phonolite diatreme, West Eifel (Germany). Mineral. Mag. 63, 615–631.
Rogelj, J., Shindell, D., Jiang, K., Fifta, S., Forster, P., Ginzburg, V., Handa, C., Kheshgi, H., Kobayashi, S., Kriegler, E., Mundaca, L., Séférian, R., Vilariño, M.V., 2018. In: Mitigation Pathways Compatible with 1.5°C in the Context of Sustainable Development. Intergovernmental Panel on Climate Change (IPCC).
Romppanen, S., 2020. The LULUCF Regulation: the new role of land and forests in the EU climate and policy framework. J. Energy Nat. Resour. Law 38, 261–287. https://doi.org/10.1080/02646811.2020.1756622.
Savant, N.K., Datnoff, L.E., Snyder, G.H., 1997. Depletion of plant-available silicon in soils: a possible cause of declining rice yields. Commun. Soil Sci. Plant Anal. 28, 1245–1252.
Schlesinger, W.H., Amundson, R., 2019. Managing for soil carbon sequestration: Let's get realistic. Global Change Biol. 25, 386–389. https://doi.org/10.1111/gcb.14478.
Schmied, M., Knörr, W., 2013. Berechnung von Treibhausgasemissionen in Spedition und Logistik gemäß DIN EN 16258. Bonn.
Schuiling, R.D., Krijgsman, P., 2006. Enhanced weathering: an effective and cheap tool to sequester CO_2. Climatic Change 74, 349–354. https://doi.org/10.1007/s10584-005-3485-y.
Schwarz, S., Freudenschuss, A., 2004. Referenzwerte für Schwermetalle in Oberböden.
Seghedi, I., Downes, H., Vaselli, O., Szakács, A., Balogh, K., Pécskay, Z., 2004. Post-collisional Tertiary–Quaternary mafic alkalic magmatism in the Carpathian–Pannonian region: a review. Tectonophysics 393, 43–62. https://doi.org/10.1016/j.tecto.2004.07.051.
Seifritz, W., 1990. CO_2 disposal by means of silicates [12]. Nature. https://doi.org/10.1038/345486b0.
Shamshuddin, J., Kapok, J.R., 2010. Effect of ground basalt on chemical properties of an ultisol and oxisol in Malaysia. Pertanika J. Trop. Agric. Sci. 33, 7–14.
Shrbený, O., 1995. Chemical Composition of Young Volcanites of the Czech Republic. Czech Geological Survey Special Paper, vol. 4. Czech Geol. Surv.
Smith, P., Davis, S.J., Creutzig, F., Fuss, S., Minx, J., Gabrielle, B., Kato, E., Jackson, R.B., Cowie, A., Kriegler, E., van Vuuren, D.P., Rogelj, J., Ciais, P., Milne, J., Canadell, J. G., McCollum, D., Peters, G., Andrew, R., Krey, V., Shrestha, G., Friedlingstein, P., Gasser, T., Grübler, A., Heidug, W.K., Jonas, M., Jones, C.D., Kraxner, F., Littleton, E., Lowe, J., Moreira, J.R., Nakicenovic, N., Obersteiner, M., Patwardhan, A., Rogner, M., Rubin, E., Sharifi, A., Torvanger, A., Yamagata, Y., Edmonds, J., Yongsung, C., 2016. Biophysical and economic limits to negative CO_2 emissions. Nat. Clim. Change 6, 42–50. https://doi.org/10.1038/nclimate2870.
Snæbjörnsdóttir, S.Ó., Sigfússon, B., Marieni, C., Goldberg, D., Gislason, S.R., Oelkers, E. H., 2020. Carbon dioxide storage through mineral carbonation. Nat. Rev. Earth Environ. 1, 90–102. https://doi.org/10.1038/s43017-019-0011-8.
Statistik Austria, 2020. Anbau auf dem Ackerland. IVEKOS.
Statistik Austria, 2018. Agrarstrukturerhebung 2016.
Steefel, C.I., Van Cappellen, P., 1990. A new kinetic approach to modeling water-rock interaction: the role of nucleation, precursors, and Ostwald ripening. Geochem. Cosmochim. Acta 54, 2657–2677. https://doi.org/10.1016/0016-7037(90)90003-4.
Stockmann, G.J., Wolff-Boenisch, D., Gislason, S.R., Oelkers, E.H., 2011. Do carbonate precipitates affect dissolution kinetics? 1: basaltic glass. Chem. Geol. 284, 306–316. https://doi.org/10.1016/j.chemgeo.2011.03.010.
Strefler, J., Amann, T., Bauer, N., Kriegler, E., Hartmann, J., 2018. Potential and costs of carbon dioxide removal by enhanced weathering of rocks. Environ. Res. Lett. 13, 34010. https://doi.org/10.1088/1748-9326/aaa9c4.
Taylor, L.L., Beerling, D.J., Quegan, S., Banwart, S.A., 2017. Simulating carbon capture by enhanced weathering with croplands: an overview of key processes highlighting areas of future model development. Biol. Lett. 13, 20160868. https://doi.org/10.1098/rsbl.2016.0868.
Taylor, L.L., Quirk, J., Thorley, R.M.S., Kharecha, P.A., Hansen, J., Ridgwell, A., Lomas, M.R., Banwart, S.A., Beerling, D.J., 2016. Enhanced weathering strategies for stabilizing climate and averting ocean acidification. Nat. Clim. Change 6, 402–406. https://doi.org/10.1038/nclimate2882.
ten Berge, H.F.M., van der Meer, H.G., Steenhuizen, J.W., Goedhart, P.W., Knops, P., Verhagen, J., 2012. Olivine weathering in soil, and its effects on growth and nutrient uptake in ryegrass (Lolium perenne L.): a pot experiment. PloS One 7, e42098. https://doi.org/10.1371/journal.pone.0042098.
Tester, J.W., Worley, W.G., Robinson, B.A., Grigsby, C.O., Feerer, J.L., 1994. Correlating quartz dissolution kinetics in pure water from 25 to 625°C. Geochem. Cosmochim. Acta 58, 2407–2420. https://doi.org/10.1016/0016-7037(94)90020-5.
Thom, J.G.M., Dipple, G.M., Power, I.M., Harrison, A.L., 2013. Chrysotile dissolution rates: implications for carbon sequestration. Appl. Geochem. 35, 244–254. https://doi.org/10.1016/j.apgeochem.2013.04.016.
Tole, M.P., Lasaga, A.C., Pantano, C., White, W.B., 1986. The kinetics of dissolution of nepheline (NaAlSiO4). Geochem. Cosmochim. Acta 50, 379–392. https://doi.org/10.1016/0016-7037(86)90191-2.
Ulrych, J., Dostal, J., Adamovič, J., Jelínek, E., Špaček, P., Hegner, E., Balogh, K., 2011. Recurrent cenozoic volcanic activity in the Bohemian Massif (Czech republic). Lithos 123, 133–144.
Ulrych, J., Lloyd, F.E., Balogh, K., 2003. Age relations and geochemical constraints of Cenozoic alkaline volcanic series in W Bohemia: a review. Geolines 15, 168–180.
Van Straaten, P., 2006. Farming with rocks and minerals: challenges and opportunities. An. Acad. Bras. Cienc. 78, 731–747. https://doi.org/10.1590/S0001-37652006000400009.
Velbel, M.A., 2009. Dissolution of olivine during natural weathering. Geochem. Cosmochim. Acta 73, 6098–6113. https://doi.org/10.1016/j.gca.2009.07.024.
Velbel, M.A., 1993. Constancy of silicate-mineral weathering-rate ratios between natural and experimental weathering: implications for hydrologic control of differences in absolute rates. Chem. Geol. 105, 89–99. https://doi.org/10.1016/0009-2541(93)90120-8.
Walker, J.C.G., Hays, P.B., Kasting, J.F., 1981. A negative feedback mechanism for the long-term stabilization of Earth's surface temperature. J. Geophys. Res. Ocean. 86, 9776–9782. https://doi.org/10.1029/JC086iC10p09776.
Washbourne, C.-L., Renforth, P., Manning, D.A.C., 2012. Investigating carbonate formation in urban soils as a method for capture and storage of atmospheric carbon. Sci. Total Environ. 431, 166–175. https://doi.org/10.1016/j.scitotenv.2012.05.037.
White, A.F., Brantley, S.L., 2003. The effect of time on the weathering of silicate minerals: why do weathering rates differ in the laboratory and field? Chem. Geol. 202, 479–506. https://doi.org/10.1016/j.chemgeo.2003.03.001.
Wild, B., Daval, D., Beaulieu, E., Pierret, M.C., Viville, D., Imfeld, G., 2019. In-situ dissolution rates of silicate minerals and associated bacterial communities in the critical zone (Strengbach catchment, France). Geochem. Cosmochim. Acta 249, 95–120. https://doi.org/10.1016/j.gca.2019.01.003.
Wilson, M., Downes, H., Cebria, J.-M., 1995. Contrasting fractionation trends in coexisting continental alkaline magma series; Cantal, Massif Central, France. J. Petrol. 36, 1729–1753.
Wilson, S.A., Harrison, A.L., Dipple, G.M., Power, I.M., Barker, S.L.L., Mayer, K.U., Fallon, S.J., Raudsepp, M., Southam, G., 2014. Offsetting of CO2 emissions by air capture in mine tailings at the Mount Keith Nickel Mine, Western Australia: rates, controls and prospects for carbon neutral mining. Int. J. Greenh. Gas Control 25, 121–140.
Wolff-Boenisch, D., Gislason, S.R., Oelkers, E.H., 2006. The effect of crystallinity on dissolution rates and CO2 consumption capacity of silicates. Geochem. Cosmochim. Acta 70, 858–870. https://doi.org/10.1016/j.gca.2005.10.016.
Wolff-Boenisch, D., Gislason, S.R., Oelkers, E.H., Putnis, C.V., 2004. The dissolution rates of natural glasses as a function of their composition at pH 4 and 10.6, and temperatures from 25 to 74°C. Geochem. Cosmochim. Acta 68, 4843–4858. https://doi.org/10.1016/j.gca.2004.05.027.
Workman, M., Dooley, K., Lomax, G., Maltby, J., Darch, G., 2020. Decision making in contexts of deep uncertainty - an alternative approach for long-term climate policy. Environ. Sci. Pol. 103, 77–84. https://doi.org/10.1016/j.envsci.2019.10.002.
Wörner, G., Schmincke, H.-U., 1984. Mineralogical and chemical zonation of the Laacher see tephra sequence (east eifel, W. Germany). J. Petrol. 25, 805–835.
Yi, H., Xu, G., Cheng, H., Wang, J., Wan, Y., Chen, H., 2012. An overview of utilization of steel slag. Procedia Environ. Sci. 16, 791–801. https://doi.org/10.1016/j.proenv.2012.10.108.
Klimaschutzbericht, 2019. Umweltbundesamt GmbH, Wien.